International Journal of
Molecular Sciences

MDPI

Review

Analysis of Factors Affecting 5-ALA Fluorescence Intensity in Visualizing Glial Tumor Cells—Literature Review

Marek Mazurek *, Dariusz Szczepanek, Anna Orzyłowska and Radosław Rola

Chair and Department of Neurosurgery and Pediatric Neurosurgery, Medical University of Lublin, 20-954 Lublin, Poland; dariusz.szczepanek@umlub.pl (D.S.); a.m.orzylowska@gmail.com (A.O.); rola.radoslaw@gmail.com (R.R.)

* Correspondence: marekmazurek@hotmail.com; Tel.: +48-81-724-41-76

Abstract: Glial tumors are one of the most common lesions of the central nervous system. Despite the implementation of appropriate treatment, the prognosis is not successful. As shown in the literature, maximal tumor resection is a key element in improving therapeutic outcome. One of the methods to achieve it is the use of fluorescent intraoperative navigation with 5-aminolevulinic acid. Unfortunately, often the level of fluorescence emitted is not satisfactory, resulting in difficulties in the course of surgery. This article summarizes currently available knowledge regarding differences in the level of emitted fluorescence. It may depend on both the histological type and the genetic profile of the tumor, which is reflected in the activity and expression of enzymes involved in the intracellular metabolism of fluorescent dyes, such as PBGD, FECH, UROS, and ALAS. The transport of 5-aminolevulinic acid and its metabolites across the blood–brain barrier and cell membranes mediated by transporters, such as ABCB6 and ABCG2, is also important. Accompanying therapies, such as antiepileptic drugs or steroids, also have an impact on light emission by tumor cells. Accurate determination of the factors influencing the fluorescence of 5-aminolevulinic acid-treated cells may contribute to the improvement of fluorescence navigation in patients with highly malignant gliomas.

Keywords: 5-aminolevulinic acid; high-grade glioma; glioblastoma; intraoperative navigation

Citation: Mazurek, M.; Szczepanek, D.; Orzyłowska, A.; Rola, R. Analysis of Factors Affecting 5-ALA Fluorescence Intensity in Visualizing Glial Tumor Cells—Literature Review. *Int. J. Mol. Sci.* **2022**, *23*, 926. https://doi.org/10.3390/ijms23020926

Academic Editor: Kiryl D. Piatkevich

Received: 15 December 2021
Accepted: 13 January 2022
Published: 15 January 2022

1. Introduction

Gliomas are among the most common tumors found in neurosurgery. It is estimated that they constitute 30% of all brain tumors and as much as 80% of malignant lesions [1]. The standard of care for malignant gliomas is maximal tumor resection, followed by radio- and chemotherapy [2]. Unfortunately, despite appropriate treatment, these tumors are prone to recurrences and have an unfavorable prognosis [3–5]. One of the reasons for this phenomenon is the high migratory ability of glioma cells, which renders the gross total resection (GTR) highly unlikely [6,7]. The analyses performed showed the presence of tumor cells up to 4 cm from macroscopically visible tumor margins [8,9]. An incomplete resection results in higher risk of neoplasm recurrence and poorer effectiveness of adjuvant therapies, such as radio- and chemotherapy [10–15]. For this reason, much attention is paid to the improvement of surgical techniques that help to maximize the percentage of achieved GTR. One of them is intraoperative fluorescence navigation that facilitates intraoperative visualization of the neoplastic tissue through the administration of substances that make it fluoresce [16,17].

Currently, a few substances are used as fluorescent indicators in brain tumor surgery. The most commonly used dye is 5-aminolevulinic acid (5-ALA) [18–20]. This compound participates in the heme metabolic pathway [21–23]. Usually, it is administered orally to patients in the form of an aqueous solution at a dose of 20 mg/kg body weight, about 3 h before the planned surgery [24,25]. Thereafter, in the body it is metabolized to the heme precursor—protoporphyrin IX (PpIX) [25–27]. This compound has two unique features

that allow it to be used in fluorescence navigation. One of them is the ability to emit a light wave after excitation by blue-violet light with a wavelength of 375–440 nm. This allows for intraoperative imaging of its deposits thanks to the use of an operating microscope with a special set of filters [19,21,23,28–30]. The second unique feature of the dye is its selective accumulation in high-grade glioma cells compared with normal brain tissue. This allows the surgeon to determine the likely margins of the operated lesion while the procedure is still ongoing. Data available in the literature indicate high specificity (83.8–93.9%) and sensitivity (73.9–91.4%) presented by 5-aminolevulinic acid [31–40].

The first studies on the usefulness of 5-ALA in high-grade glioma surgery were carried out in the 1990s [21,22]. Since then, the use of this dye has been repeatedly demonstrated to improve the percentage of GTR achieved in glioblastoma patients by using intraoperative fluorescence navigation [19,24,29,41–44]. Additionally, as a meta-analysis by Gandhi et al. shows, this also results in progression-free survival and survival rates of the patients [18]. However, the presence of fluorescence and its nature are not the same for all glial tumors. Many times, despite the supply of an appropriate dose of dye in the appropriate time window, no fluorescence is observed after the tumor is visualized, which significantly hinders the course of the procedure. The goal of this study is a literature review on the topic of the factors affecting the mechanism of fluorescence induced by the supply of 5-aminolevulinic acid.

2. Intracellular Metabolism of 5-Aminolevulinic Acid

When considering the metabolism of 5-ALA and its potential influence on the strength of fluorescence, one should remember that the cell can derive 5-ALA from two sources. The first one is the exogenous supply. The dye is administered orally to patients; then it is absorbed from the digestive tract and distributed throughout the body. Exogenous 5-ALA is delivered to cells via special transporter proteins. This group includes peptide transporter 1 (PEPT1) and peptide transporter 2 (PEPT2) [45,46]. The other source of the dye is its endogenous fraction, produced from succinyl-CoA and glycine. This process takes place in the mitochondria and is catalyzed by ALA synthase (ALAS) [46–49]. Then, endogenous 5-ALA is transported to the cytoplasm, where it can undergo further transformations together with the exogenous fraction.

The first steps occur in the cytoplasm, while the final transformations take place in the mitochondria [50]. In the first act of metabolism, two 5-ALA molecules condense to porphobilinogen (PBG) in a reaction catalyzed by ALA dehydratase (ALAD). Another name for this enzyme is porphobilinogen synthase (PBGS). Then, porphobilinogen deaminase (PBGD), also known as hydroxymethylbilane synthase (HMBS), catalyzes the fusion reaction of four PBG molecules, resulting in the formation of hydroxymethylbilane (HMB). Its structure is later closed by uroporphyrinogen III synthase (UROS) to form the cyclic uroporphyrinogen III. The next step is its decarboxylation. This reaction is catalyzed by uroporphyrinogen III decarboxylase (UROD), and its product is coproporphyrinogen III. The next stages of metabolism take place already in the mitochondria. The transport of metabolites is mediated by ATP-binding cassette transporter B6 (ABCB6). In mitochondria, coproporphyrinogen III oxidase (CPOX) catalyzes the oxidative decarboxylation of coproporphyrinogen III, resulting in the formation of protoporphyrinogen III. It is further oxidized to protoporphyrinogen IX (PpIX) by protoporphyrinogen III oxidase (PPOX). It is protoporphyrinogen IX that is the main source of fluorescence used in intraoperative 5-ALA navigation. In the last step, Fe^{2+} is included in the pyrrole ring of PpIX. As a result, nonfluorescent heme is formed. This process also takes place in the mitochondria and is catalyzed by ferrochelatase (FECH). Additionally, reaction can be accelerated by heme oxygenase-1 (HO-1) [48,50–57]. If heme and free porphyrin metabolites remain inside the cells for a long time, they can induce oxidative stress and damage them. For this reason, a well-coordinated mechanism of their further transport and degradation is very important [58]. The ATP-binding cassette subfamily G (ABCG) 2 protein [59–61] plays a

key role in their transmembrane transport. Intracellular metabolism of 5-ALA is shown schematically in Figure 1.

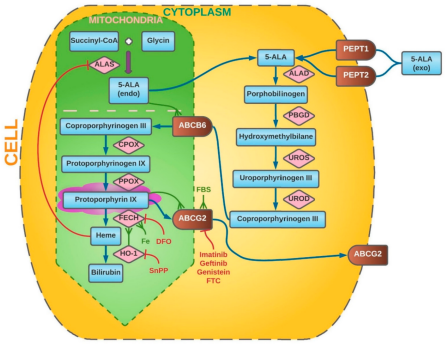

Figure 1. Intracellular metabolism of 5-ALA. The synthesis steps of heme metabolism are labelled by blue arrows (↑). Red indicators (T) point to enzymes and substances that inhibit particular steps of metabolism, whereas green indicators (Ψ) highlight factors that promote them. PEPT 1/2—peptide transporter 1/2, ALAS—ALA synthase, ALAD—ALA dehydratase, PBGD—porphobilinogen deaminase, UROS—uroporphyrinogen III synthase, UROD—uroporphyrinogen III decarboxylase, ABCB6—ATP-binding cassette transporter B6, CPOX—coproporphyrinogen III oxidase, FECH—ferrochelatase, ABCG 2—ATP-binding cassette subfamily G 2 Protein, DFO—deferoxamine mesylate, FBS—fetal bovine serum, SnPP—tin protoporphyrin IX, FTC—fumitremorgin C, 5-ALA (endo)—endogenous 5-ALA, 5-ALA (exo)—exogenous 5-ALA.

3. Alterations in 5-Aminolevulinic Acid Metabolism in Neoplasm Cells

The heme metabolic pathways described above differ between normal and neoplastic cells, resulting in a variation in fluorescence. The reason is both the greater accumulation of PpIX inside the cancer cells and the reduced rate of its transformation. This discrepancy may result from the difference in the rate of division between neoplastic and healthy cells [62,63]. This applies, inter alia, to porphobilinogen deaminase, the activity of which increases during replication [64–66]. It was confirmed that the higher activity of this protein concerns rapidly dividing cells, including tumors [64,67–73]. The increase in PBGD activity may be caused by the administration of 5-ALA itself [74,75]. However, no association has been demonstrated between higher PBGD activity and PpIX accumulation [74,76]. On the other hand, studies on esophageal cancer cells have suggested a correlation between high PBGD activity and decreased FECH function, which could result in increased PpIX accumulation [71]. Further observations did not confirm the existence of this relationship though [64,68,72]. Other enzymes involved in heme metabolic changes are also more active in neoplastic tissues. Greater UROS expression was noted in breast cancer and in tumor biopsies from head and neck cancer patients [73,77]. Another enzyme with altered activity in cancer cells is ferrochelatase. Reduced FECH expression has been demonstrated in many tissues and tumors, including glioblastoma multiforme [64,72,78–80]. This condition promotes longer accumulation of PpIX inside cells, which may also be related to the intensity of their fluorescence [78,81–83]. However, this phenomenon also applies to other gliomas, including LGG. Studies by Teng et al. showed a decreased level of FECH mRNA expression in glioblastoma, diffuse astrocytoma, and anaplastic astrocytoma cells compared with normal tissue. It is worth noting, however, that the lowest values were for malignant WHO IV tumors [84]. Cancer cells can also be distinguished by the production of endogenous 5-ALA. The key enzyme in this process is ALA synthase (ALAS). Colorectal cancer specimens showed a significantly lower activity of this enzyme compared with normal tissue [78]. However, in the case of lung cancer, the opposite trend was observed [85]. Still, there are no data in the literature regarding ALAS activity in glioblastoma cells.

Neoplastic cells are characterized by differences not only in the activity of enzymes in the hem metabolism pathway but also in the activity of hem transporters and their metabolites. PEPT2, the major protein responsible for transporting 5-ALA into the cell interior,

has been shown to be overexpressed in glioblastoma cells [84]. Analogue discrepancy applies to ABCG2, which is also an intermembrane transporter of hem metabolites [86–88]. ABCB6 is another transporter belonging to the same family of proteins. Zhao et al. noted that it may also affect the distribution of PpIX. Their studies on glioblastoma cells showed higher expression of this protein in glioma cells compared with normal brain tissue, but the intracellular localization of ABCB6 does not provide unambiguous evidence regarding its influence on the degree of PpIX accumulation [89–92]. However, the above-presented discrepancies in the metabolism and transport of heme metabolites result in greater accumulation of PpIX in some tumor cells, which is a key aspect used in fluorescence intraoperative navigation [22,93]. Additionally, studies by Stummer et al. in a rat model showed that glioblastoma cells metabolize 5-ALA and collect its excess both in vivo and in vitro, which may interfere with the detection of fluorescence [22]. The heme metabolism is subject to natural regulatory processes. The availability of substrates and intermediates plays an important role in it. An important regulating point is, inter alia, inhibition of ALAS in the feedback mechanism [94]. It can be inhibited directly by the intracellular heme level [95]. However, this compound also influences other stages of metabolism, including the rate of its degradation by heme oxidase [50,83].

However, PpIX fluorescence after exogenous 5-ALA supply is not a common feature of all neoplastic cells. It has been shown many times that it concerns mainly cells exhibiting marked features of malignancy. It is clear that the use of fluorescent intraoperative navigation shows the significant effectiveness of this method in the treatment of patients with high-grade glioma (HGG) [19,24,29,41–43,96–99]. However, for low-grade glioma (LGG), the statistics are not that promising. One of the first reports on the use of 5-ALA in the surgery of low-grade gliomas comes from Ishihara et al. The authors, examining 65 slices from six resected tumors, showed that diffuse astrocytomas exhibit noticeably weaker PpIX fluorescence compared with anaplastic astrocytomas and glioblastoma [100]. This was in line with the later work of Widhalm et al., who showed no light emission for 100% (8/8) of the samples from patients with WHO grade II diffusely infiltrating gliomas [101]. Their later work confirmed these initial observations—of the 215 tumor specimens analyzed from 59 patients with diffusely infiltrating gliomas, only 19% (4/33) of the WHO II tumor samples showed noticeable fluorescence. For comparison, in WHO grade III gliomas, focal PpIX fluorescence was visible in 85% (23/26) of the cases [102]. A similar inconsistency was visible in the insights of Ewelt et al., who detected visible PpIX fluorescence only in 7.7% (1/13) of WHO II glioma and 70.6% (12/17) of higher-grade tumors [32]. Observations on a larger group of patients were conducted by Wadiur et al. The authors analyzed the presence of fluorescence in 110 patients with low-grade glioma tumors in imaging studies and recorded it in 36% (40/110) of the cases. Moreover, subsequent analysis of the results of histopathological examinations revealed that of the WHO II tumors, only 11% (7/65) showed noticeable luminosity. In the case of WHO III and WHO IV tumors, it was 68% (26/38) and 100% (7/7), respectively [103]. Similarly, Jaber et al. in their study proved that of 166 eligible tumors (82 WHO II, 76 WHO III, and 8 WHO IV), PpIX fluorescence was present in more malignant tumors. The authors concluded that if the lesion fluoresces, it is HGG 85% of the time. For LGG, the percentage of glowing tumors was 16% (13/82) [104]. The problem with visualizing pure low-grade glioma fluorescence was also reported by other authors [27,105–110]. However, there are case reports of LGG patients showing visible fluorescence [111,112]. Moreover, Marbacher et al. confirmed the presence of detected glow in 40% (8/20) of the analyzed LGGs [108]. Similar value results were shown by Valdés et al. Goryaynov et al. showed even greater fluorescence when out of 27 histologically confirmed tumors (14 diffuse astrocytomas, 6 oligodendrogliomas, 4 pilocytic astrocytomas, 2 gemistocytic astrocytomas, and 1 desmoplastic infantile ganglioglioma), 52% showed fluorescence after exogenous 5-ALA supply at a dose of 20 mg/kg. However, the quality of lighting was diverse—50% of the tumors showed diffuse fluorescence, and 50% focal [113,114]. Some authors suggested that such foci of increased fluorescence in low-grade glioma tissue may indicate local malignancy [114,115].

Interestingly, fluorescence heterogeneity is also frequently observed in tumors with a high proliferation rate. Many have authors shown significant discrepancy in the fluorescence intensity between different glioma cell lines subjected to the same conditions [46,57,116,117]. The phenomenon has also been observed intraoperatively. Stummer et al. noted significant regional heterogeneity in fluorescence intensity for glioblastoma tissue. It has been suggested that the reason for the different intensity of light may be a various cell density within the tumor [101,102,118]. However, it is probably caused by the significant genetic polymorphism of neoplastic cells resulting from the rate of their proliferation. This was very well outlined in a study by Kim et al., in which the authors classified samples from five patients with glioblastoma in terms of luminosity and then subjected them to a thorough RNA sequencing analysis. A total of 585 genes that influence the PpIX accumulation and fluorescence intensity were identified [80]. As previously mentioned, other authors have also suggested a relationship between the rate of cell proliferation and the luminosity [18–20]. Additionally, Widhalm et al. analyzed the role of 5-ALA in identifying anaplasia foci in diffusely infiltrating gliomas with nonsignificant contrast enhancement [101]. The results obtained by the authors showed that Ki-67/MIB-1 is significantly higher in the areas of the tumor showing PpIX fluorescence (20% vs. 10%) [101]. In their following work, the authors analyzed features of 215 tumor specimens collected from 59 patients with diffusely infiltrating gliomas with nonsignificant contrast enhancement on MRI. They showed that in fluorescent areas, mitotic rate, cell density, nuclear pleomorphism, and proliferation rate were significantly higher than in nonfluorescing areas. Similar results were presented by Ohba et al., who in their observations on 104 patients with glioma showed that contrast enhancement, WHO malignancy, IDH status, and the Ki-67/MIB-1 index influence intraoperative tumor glow assessed by the surgeon [106]. Likewise, Jaber et al. examined the influence of tumor volume, 18F-FET PET uptake, contrast enhancement, grade, IDH1 mutation status, O6-methylguanine DNA methyltransferase (MGMT) promoter methylation status, 1p/19q codeletion, and Ki-67/MIB-1 and proved that the intensity of fluorescence correlates with the expression of Ki-67 and with the grades of histological malignancy. No similar relationship was found for MGMT status, IDH1 mutation status, or 1p19q codeletion status, however [104]. Equally, Saito et al., on the basis of univariate analysis, also showed a relationship between the intensity of cell proliferation measured with the Ki-67/MIB-1 index and the luminosity induced by 5-ALA supply. It should be noted, though, that a similar relationship also occurred in the case of 1p19q codeletion status in contrast to the previously mentioned work. A work by Ishihara et al. is also worth mentioning, in which on top of the similar relationship between the Ki-67/MIB-1 index and the fluorescence intensity, it was shown that this parameter is also influenced by CD31-microvessel density and larger VEGF expression. However, a more detailed multiple regression analysis showed that only the Ki-67/MIB-1 index was significantly related to the fluorescence intensity [19]. It has been suggested that modifications of tumor metabolism related to increased cell proliferation might affect the activity of enzymes responsible for the intensity of PpIX accumulation [80,119]. Mechanisms affecting the visibility of fluorescence were induced by the supply of 5-aminolevulinic acid.

3.1. Blood–Brain Barrier

One of the factors that may influence the accumulation of dyes in cells, and hence the intensity of light, is the structure of the blood–brain barrier (BBB). It is the primary border separating the brain environment from the rest of the body. However, brain tumors can cause dysfunction and degradation, simultaneously affecting tumor growth and the effectiveness of therapeutic strategies. This is also true for fluorescent intraoperative navigation [120]. The potential for 5-ALA penetration into the brain was considered in the past, explaining the presence of neuropsychiatric symptoms in hepatic porphyria [121]. However, observations of the distribution of radiolabeled ALA by Terr and Weiner showed no penetration of the dye into the brain tissue [122]. This was in line with the conclusions of Stummer et al., who did not show the presence of fluorescence caused by 5-ALA

administration in patients with a normal blood brain barrier structure [123]. It therefore appears that under normal conditions, it is impermeable to 5-ALA [84]. On the other hand, transport via BBB was noted by McGillion et al., and a slight displacement of 5-ALA within the blood–brain barrier itself has also been shown in other studies [124,125]. Few authors have described the ability of choroid plexus to transport 5-ALA, but it has not been shown that it is able to penetrate the brain tissue [123,126,127]. Therefore, Ennis et al. analyzed the distribution of radiolabeled ALA across the blood–brain and blood–cerebrospinal fluid barrier in rats. The authors showed that in adults, the spread of the dye in the brain tissue was low and suggested that this probably took place by means of passive diffusion since the increase in plasma ALA concentration was not associated with the increase in its distribution to the brain tissue [128]. The lack of active transporters was also consistent with the results of García et al., who analyzed the structure of brain microvessels without proving the presence of transporters enabling the distribution of the dye to the brain tissue [125]. The above observations suggest that despite the possibility of interaction of 5-ALA with membrane transporters in various tissues, the blood–brain barrier in the normal state is practically impermeable to it [129–132]. Consequently, the condition necessary for the accumulation of PpIX after the exogenous supply of the dye is the state of disturbance of its structure. The severity of BBB dysfunction depends on the location, volume, type, and malignancy of the tumor [133]. In the case of gliomas, the difference in barrier permeability between LGG and HGG has been repeatedly demonstrated. While in tumors of low malignancy BBB disruption is relatively minor, in malignant gliomas it results in edema and the formation of areas with impaired vascular density and integrity [134–137]. Additionally, astrocytes migrate away from vascular endothelial cells, resulting in the disruption of a barrier structure, thereby affecting BBB permeability [138]. This may provide an explanation for the disparity in PpIX accumulation and fluorescence of lesions depending on their malignancy [28,93,120,134,139].

3.2. ABCG2 and ABCB6 Transporters

Intracellular 5-ALA transport may also have an influence on the PpIX accumulation and fluorescence intensity. The ABCG2 transporters, which as previously mentioned are crucial in the distribution of heme metabolites, play an important role in this issue. These are proteins belonging to the larger family of the ATP-binding cassette superfamily located in the plasma membrane [1,61]. Their function is not only to remove porphyrins but also to transport xenobiotics and harmful toxins outside the cell [140]. The presence of ABCG2 was first demonstrated in a study of doxorubicin-resistant breast cancer cells, which gave it its second name, breast cancer resistance protein (BCRP) [141]. Later they were found in many tissues of the body, including the blood–brain barrier, and their overexpression is a characteristic feature of many cancers [30,87,88,142–149]. Moreover, their expression level corresponds to the histological grade of neoplastic lesions [88]. It has been shown that high activity of ABCG2 is associated with a decrease in intracellular accumulation of PpIX after ALA administration, which results in a lower intensity of fluorescence [60,149]. Moreover, the fact that blocking ABCG2 receptors causes the accumulation of porphyrins and ABCG2 blocking with imatinib and gefitinib increases the effectiveness of photodynamic therapy have already been shown [150–153]. This type of transporter can also be blocked by genistein [154]. Reiner et al. observed the fluorescence intensity in three different GBM cell lines and found no effect of genistein on the intensity of endogenous PpIX glow. However, after 5-ALA was added to the cell lines, there were significant discrepancies due to dye accumulation. The simultaneous application of genistein and 5-ALA increased PpIX fluorescence by 42% for U87MG cells, by 31% for U87wtEGFR cells, and by 54% for U87vIII cells compared with the use of 5-ALA alone [155]. This phenomenon was also observed in studies by Piffaretti et al., which showed the effect of increasing genistein concentrations on the viability of the analyzed glioblastoma cell lines. Moreover, they also noticed an increase in fluorescence of cells incubated in genistein and 5-ALA media compared with 5-ALA alone [46]. A number of other compounds are also known that

may affect the expression level and function of ABCG2 transporters, thereby affecting the intensity of PpIX fluorescence, such as Ko143 or flavonoids, including 6-prenylchrysis and tectochrysin [156–159]. Currently, there are no studies of the impact of their application on the fluorescence intensity in gliomas though. It is worth mentioning that the fluorescence intensity and transport activity can be influenced not only by chemical but also by physical factors. Recent studies on breast cancer stem cells have shown that ultrasound has the effect of reversing chemoresistance by altering the expression of ABCG2 [160]. Interesting conclusions were also brought by a research conducted by Higuchi et al. The authors analyzed the effect of ultrasound on the intensity of fluorescence of cells and on the expression of ABCG2 after 5-ALA administration. It was shown that exposure of the cells to 5-ALA caused a slight increase in the expression of the transporters; however, this effect was suppressed by ultrasounds that reduced the expression of ABCG2. The increase in the intracellular accumulation of PpIX in glioblastoma cells was confirmed by a spectrometer. This applied to all analyzed cell lines, and the effect lasted for over 2 h with some differences in the intensity and dynamics of the increase in glow between different cell populations [161]. It should be mentioned, however, that the inhibition of ABCG2 was not associated with an increase in PpIX accumulation in all observations. Wang et al. used reserpine to lower ABCG2 activity in their study on glioma cancer stem cells (GSCs) and showed that it did not improve the PpIX fluorescence in both the group of GSCs and the control group. Moreover, in the case of GSCs, the effect was even lower accumulation of PpIX [162]. This may be due to the influence of reserpine on other ABC family transporters present in the cell: ABCB6, ABCB7, and ABCB10. Disruption of their function may impair PpIX metabolism, contributing to its lower accumulation in cells [162,163]. However, the abovementioned data show that the regulation of the function of ABCG2 transporters has a great potential to modify PpIX accumulation and tumor cell fluorescence during intraoperative navigation. One should remember yet that long-term administration of ABCG2 inhibitors may be associated with phototoxicity reactions and the disruption of transporters in other parts of the body, such as kidneys, which may have negative consequences for patients [164,165]. Therefore, further observations in this matter are needed in order to develop an optimal strategy for a potential treatment.

Other proteins from the ATP-binding cassette superfamily family may also influence heme transformation processes. In recent years, the role of the ABCB6 protein transporter in the regulation of PpIX metabolism in leukemic cells has been demonstrated [166]. As mentioned before, this protein is responsible for the transport of coproporphyrinogen from the cytoplasm to the mitochondria in order to carry out further changes in the heme synthesis pathway [166]. Zhao et al. in their study analyzed ABCB6 expression in surgical glioma samples and proved a much higher expression of ABCB6 mRNA compared with normal brain tissue. Moreover, this increase correlated with the histological grade of the tumor. WHO IV cells showed the highest expression, but a statistically significant difference was already visible in WHO II cells, compared with normal brain tissue. In the next step, the authors showed that cells with high abundance of ABCB6 were also characterized by higher dye accumulation and higher fluorescence intensity and proved that incubation with exogenous ALA resulted in a further increase in ABCB6 expression [89]. Additionally, cells overexpressing ABCB6 showed a higher level of PpIX accumulation compared with control cells. In the last stage of the study, the authors checked whether inhibition of ABCB6 with a specific siRNA would cause a change in the intensity of dye accumulation. The results showed that ABCB6 expression silencing was associated with a significant decrease in accumulated PpIX in comparison with control cells. The data obtained from the study showed that the above-described phenomena apply only to cells exposed to exogenous 5-ALA [89]. The exact mechanism by which the increase in ABCB6 expression leads to increased PpIX accumulation has not been described to date.

Interestingly, it is not only ABCG2 transporters that can influence the efflux of PpIX from cells. Kitajima et al. conducted a study in which they analyzed the distribution of PpIX in cells derived from the JFCR39 panel. It is a panel consisting 39 human cancer cell

lines from nine different tissues (lung, colon, gastric, breast, ovarian, brain, renal, prostate cancer, and melanoma) established by the Japanese Foundation for Cancer Research. The analysis studied the effect of the known ABCG2 inhibitor fumitremorgin C (FTC). In most of the cells of the JFCR39 panel, FTC administration increased the intracellular accumulation of PpIX and decreased its extracellular fraction, which was related to the inhibition of ABCG2 [167]. These results were consistent with the observations of other authors [59,168,169]. Nevertheless, this trend was not true for all of the lines included in the study since some of them showed no strong correlation between the level of dye excretion and ABCG2 expression. Surprisingly, a much stronger correlation was found in the case of the expression of the protein involved in exocytosis, which is dynamin 2. Additionally, inhibition of dynamin 2 significantly increased the accumulation of PpIX by limiting the excretion of the dye [167]. It may be beneficial to perform subsequent observations on glioblastoma cells in order to better understand this mechanism.

3.3. Activity of Ferrochelatase (FECH)

Another point of key importance in the accumulation of PpIX is the incorporation of Fe^{2+} into its pyrrole ring, resulting in the formation of nonfluorescent heme. This reaction is catalyzed by ferrochelatase (FECH), a homodimer composed of two amino acid polypeptide chains, located in the mitochondrial membrane [55,78,170,171]. It has been shown that molecular defects or low expression of FECH results in a lower dye content [62,172]. As mentioned earlier, the cells of many neoplasms are characterized by reduced activity of this enzyme [53,80]. This results in a lower conversion rate of PpIX to nonfluorescent heme and hence a higher glow intensity [81,83]. Importantly, the reduction of the activity of FECH may then contribute to an increase in PpIX accumulation inside cells, which has been proven in colorectal and cancer cells. A similar issue, therefore, became the subject of a research by Teng et al. conducted on both human glioma cell lines and surgical specimens. The authors proved that glioblastoma has a prominent downregulation of FECH mRNA expression when compared with normal brain. Other types of gliomas also showed lower albeit less pronounced expression. In addition, inconsistency between different cell lines was also found. The G112 line had the highest expression of ferrochelatase mRNA, while the U87 line had the lowest. This reflected the disproportion in fluorescence after the supply of exogenous 5-ALA with the highest intensity in the case of the U87 line, and the lowest for G112 and SNB19 lines. Moreover, the authors affected FECH activity by siRNA in two cell lines with silencing efficacy greater than 50% for both lines. This resulted in the intracellular accumulation of PpIX and increased intensity of fluorescence in cells exposed to 5-ALA, proving that the use of small RNA interference may allow for a significant increase in the quality of fluorescence achieved [84]. Similar studies on the silencing of the FECH gene were also conducted on other neoplasms [78,84,172,173].

It is worth remembering that other factors may also influence ferrochelatase activity. The natural form of its regulation is the availability of free Fe^{2+} ions [57,63]. Deferoxamine mesylate (DFO) is a compound commonly used in clinical practice for the treatment of cutaneous porphyria. It exerts its effect on blocking FECH activity by chelating iron ions so that they cannot be introduced into the pyrrole ring of PpIX [46,174–176]. The result is an increase in the intracellular volume of PpIX and a greater intensity of fluorescence. Hence, an increase in dye accumulation under the influence of DFO has been demonstrated in various neoplastic cells, including glial ones [177–183]. Reiner et al. analyzed the effect of deferoxamine on three glioblastoma cell lines. The results showed that the supply of DFO in the absence of 5-ALA did not affect the luminance. However, among cells previously exposed to the dye, significant increase in glow intensity was observed in all analyzed cell lines and varied from 6% for U87wtEGFR to 22% for U87vIII lines, respectively, compared with cells treated alone [155]. It was consistent with the observations of other authors. Valdes et al. analyzed the effect of DFO supply in studies conducted on mice implanted with xenograft U251-GFP glioma tumor cells. The animals took a dose of deferoxamine for 3 days and then were given 5-ALA to induce fluorescence. The results showed a 50%

increase in PpIX fluorescence intensity in the group of animals receiving DFO compared with the control group. The reported glow level after dye administration was 2.9 times greater than the background in mice treated with DFO, and only 1.9 times greater in the control group [184]. Another interesting conclusion can be drawn from studies by Wang et al. on glioma cancer stem cells (GCSs). The authors showed that the addition of DFO to cells exposed to ALA increased the accumulation of PpIX. This effect was visible both in GCS cells and in the control group [162]. These observations show the great potential of deferoxamine in increasing the fluorescence intensity. However, it should be mentioned that for some authors the results were not as promising. A study by Choudry et al. showed no greater accumulation of PpIX in basal cell carcinoma patients after exposure to DFO [185].

3.4. Function of Heme Oxygenase (HO-1)

Another compound involved in the heme homeostasis is heme oxygenase-1 (HO-1), which is responsible for the conversion of heme into biliverdin, carbon monoxide, and Fe^{2+} ions [186–189]. The high activity of HO-1 results in a large production of Fe^{2+} ions, which, as we mentioned earlier, are the regulating point of FECH efficiency. Moreover, the rapid depletion of heme itself may alter the enzymatic activity in favor of increased PpIX metabolism by FECH. The effect is an increase in the rate of heme synthesis from Fe^{2+} and PpIX, which reduces the intensity of the fluorescence of cells [57,106,162,190,191]. Importantly, this enzyme has been shown to be overexpressed in many conditions that affect the CNS, such as ischemia, brain injuries, or Alzheimer's disease [192–194]. There are also data in the literature showing the upregulation of HO-1 in many neoplasms, such as kidney, prostate, and lung cancer; squamous cell carcinoma of the oral cavity; melanoma; Kaposi's sarcoma; lymphosarcoma; hepatoma; and chronic myeloid leukemia [195–203]. This also applies to brain tumors, including gliomas [204,205]. Moreover, an association was noted between HO-1 expression and tumor progression and its histological grade. Paradoxically, Andaloussi et al. showed that an increase in tumor malignancy is associated with a higher expression of HO-1, which should translate into lower accumulation of PpIX [204,206]. Convergent conclusions were also seen in the work of Gandini et al. The authors showed a significant difference in the expression of HO-1 between glioblastoma and normal brain tissue (54% vs. 22%). The expression level was increased in all analyzed grades and histological subtypes. However, no changes in HO-1 levels were shown with increasing tumor grade. In addition, the authors also noted a significant reduction in survival in patients with WHO grade II and III astrocytoma with high HO-1 expression. It concerned only the cytoplasmic localization of the enzyme [207].

The previously mentioned studies by Wang et al. focused on the observation of enzyme expression in a population of glioma cancer stem cells (GCSs) [162]. These are cells characterized by properties responsible for the initiation of the neoplastic process, often related to the tumor resistance to conventional treatments [208,209]. The observations of Wang et al. showed that the GCSs showed a lower level of fluorescence compared with the cells from the control group following exposure to 5-ALA (34.9% $\pm$ 5.4% of the GCSs vs. 68.1% $\pm$ 12.6% cells in the control group). When the authors analyzed the level of HO-1 expression, they found that the level of expression of this enzyme in GSCs is high, which results in a lower accumulation of PpIX and, hence, a lower intensity of fluorescence [162]. Data linking high HO-1 expression with decreased PpIX accumulation were provided, inter alia, through studies carried out on melanoma cells. Moreover, the authors showed that enzyme inhibition causes an increase in fluorescence intensity [210]. Similar attempts to enhance the fluorescence of tumor cells by inhibiting the activity of HO-1 were also made in gliomas. The studies conducted by Piffarett and Reiner et al. investigated the effect of tin protoporphyrin IX (SnPP, a synthetic heme analogue with a tin atom in the core) on the intensity of fluorescence induced by 5-ALA supply in glioblastoma cell lines. Due to its structure, SnPP inhibits the activity of HO-1 and is commonly used in pediatric patients suffering from hyperbilirubinemia [211]. Fluorescence intensity analysis showed that the simultaneous use of SnPP and 5-ALA allows for increasing the glow intensity.

Moreover, the increase differs between cell lines from 39% for U87wtEGFR to 81% for U87MG. Interestingly, an even greater difference in the light intensity was present with the supply of SnPP alone [46,155]. This relationship may be related to EGFR expression. U87MG cells have normal EGFR expression, while U87wtEGFR overexpresses EGFR, and U87vIII cells express the EGFR version III mutation (EGFRvIII) [46,155].

EGFR, a member of the ErbB receptor family, is an important element in the regulation of cell growth in tissues of epithelial origin [44,212]. Recent studies have shown its key role in tumorigenesis, cell migration, and angiogenesis. Upon binding of a specific ligand, intracellular tyrosine kinase is activated, which leads to the activation of signaling along the Akt, PI3 kinase, and nuclear factor (NF-kβ) proteins pathways. The result is a decrease in cell apoptosis, an increase in proliferation and angiogenesis, and a greater tendency to migrate [2,44,212–214]. The mutation present in EGFRvIII cells is characteristic of GBM since 40% of glioblastoma cells have a mutation that overexpresses EGFR, of which about 50% is the EGFRvIII variant, which results in uninterrupted activity of the receptor without the need for external stimulation [215–220]. The abovementioned experiments clearly indicate a relationship between the function of HO-1 and the activity of the epidermal growth factor receptor. The presence of a similar relationship has already been observed in non-small cell lung cancer and colon cancer. Studies have shown that EGF stimulation, through NF-kβ activation, contributes to an increase in HO-1 and can be induced by various pathways, such as PI3K, IKK, and protein kinase C (PKC) [221–223]. Likewise, Fontana et al. focused their research on the analysis of the influence of EGFR activity on HO-1 function in glioma cell lines: U87MG (low EGFR expression), LN229EGFR (EGFR overexpression), and BS153 (EGFRvIII mutation). Initially, all lines were exposed to 5-ALA, and their fluorescence was checked. BS151 cells were characterized by the weakest intensity of light, which was probably related to the constitutively active EGFRvIII +. In the next step, EGF was added to the samples. The result was a significant decrease in fluorescence for U87MG and LN229EGFR, while no significant change was observed in BS153 culture. This effect was reversed by EGFR-specific siRNA, which reduced protein expression by approximately 80% in U87MG. The authors suggested that this was related to EGFR receptor activation, which resulted in the promotion of HO-1 transcription and expression in a concentration-dependent manner. The mutant BS153 cell receptor remained uninterruptedly active with no effect upon the addition of EGF. To test this theory, the authors inhibited the effect of HO-1 by using SnPP (HO-1 inhibitor) and HO-1-specific siRNA. In both cases, the effect was to restore fluorescence in all cell lines, independent of EGFR expression. Additionally, gefitinib, which is a selective inhibitor of the EGF tyrosine kinase receptor, was added to lines previously exposed to EGF. As a result, the fluorescence was restored in U87MG cells, but no effect was obtained in the case of BS153 [57]. These data clearly indicate a strong relationship between EGFR and HO-1 activity. It also suggests a potential cause of inhomogeneous fluorescence in some tumors composed of cells characterized by intratumoral heterogeneity of EGFR/EGFRvIII, which may make it very difficult to determine the extent of resection [116,224].

3.5. Significance of Isocitrate Dehydrogenase (IDH) Status

Other genetic features of tumors may also influence their susceptibility to PpIX accumulation-dependent fluorescence. The new classification of tumors of CNS created by the World Health Organization (WHO), in addition to the standard four-step division according to the degree of histological malignancy, also included a group of neoplasms in which the key role is played by the mutant isocitrate dehydrogenase (IDH) 1/2 [225]. It is widely believed that the IDH1/2 mutation occurs at one of the early stages of gliomagenesis. As a consequence, there are two different pathways of neoplastic cell progression depending on the mutation status [226]. Some authors have even suggested that these discrepancies in the origin of the cells may also affect their ability to fluoresce. It should be noted that, physiologically, isocitrate dehydrogenase 1 is one of the enzymes involved in the Krebs cycle. Its role is to catalyze the oxidative decarboxylation of isocitrate to α-ketoglutarate

(α-KG) with simultaneous conversion of NADP (+) to NADPH in the cytoplasm and peroxisomes [227,228]. As mentioned earlier, endogenous ALA synthesis depends on the availability of glycine and succinyl-coenzyme A being the reactants [46–49,229,230]. This indicates a possible role for IDH in regulating PpIX metabolism. IDH1 mutations are present in 55% of WHO III gliomas and 6% of WHO IV [231]. Their presence causes a decrease in the physiological activity of the enzyme, with the simultaneous production of R-2-hydroxyglutarate (2-HG) through the consumption of NADPH, which is an oncometabolite favoring neoplastic transformation [232–235].

In their research, Ohba et al. analyzed 104 patients operated on for glioma for factors that could affect the fluorescence of the tumor tissue exposed to 5-ALA. Analysis of the collected data showed that among glial tumors, cells with the IDH1/2 mutation showed less fluorescence compared with cells without this mutation. Interestingly, this relationship concerned both high- and low-grade glial tumors. Additionally, in order to find out about the nature of this phenomenon, the authors analyzed the glow intensity of two glioma cell lines in vitro: NHAE6E7hTERTIDH1mut, which was transformed by mutant IDH1, and NHAE6E7hTERTRas, which was transformed by H-Ras (wild-type IDH1 model). Both lines were exposed to 5-ALA. Then, the accumulation of PpIX in both cell types was assessed. The authors showed that the concentration of the dye was lower in NHAE6E7hTERTIDH1mut than in NHAE6E7hTERTRas. This confirmed the genetic basis for the difference in cell fluorescence depending on the IDH1/2 mutation status. The authors suggested that a potential reason for this relationship is the greater activity of FECH and HO-1 in mutant cells, which results in an increase in PpIX metabolism and its lower accumulation [106]. Similar conclusions were drawn by Hickman et al. They analyzed 58 patients with HGG operated under the guidance of intraoperative fluorescence navigation using 5-ALA. The results showed a statistically significant predominance of tumors with an IDH mutation in the group of nonfluorescent lesions—70.6% of tumors with and 100.0% without IDH mutation showed PpIX fluorescence [236]. The presented data were consistent with the results of other authors. In their observations on 60 patients with astrocytic or oligodendroglial tumors, Saito et al. studied the effect of IDH1 status, 1p19q loss of heterozygosity (LOH), the MIB-1 labelling index, the tumor margin, heterogeneity, and contrast enhancement on MRI scans. The authors showed that only the status of isocitrate dehydrogenase 1 allowed for predicting the fluorescence of the tested cells to a statistically significant degree. Their data indicated that only 15% of the cells with the IDH1 mutation showed intraoperative florescence induced by 5-ALA administration [109]. On the other hand, Jaber et al., who also studied the factors influencing the fluorescence of cells after 5-ALA administration, did not show any correlation between the intensity of fluorescence and IDH1, 1p/19q, and MGMT promoter methylation status. It should be noted, however, that the study was deliberately selected for glial tumors not showing radiological features characteristic of glioblastoma multiforme. Out of 166 samples, postoperative histopathological examination revealed 82 WHO II, 76 WHO III, and 8 WHO IV tumors [104].

The role of IDH1 in PpIX metabolism was also investigated by Kim et al., whose cohort included tumor samples from 5-ALA fluorescence-guided surgeries in 35 patients with WHO III gliomas. Postoperative examination of tumor samples revealed the presence of IDH1 mutations in 24 of them, of which 16 showed luminosity. The authors showed a statistically significant relationship between the presence of a mutation and tumor fluorescence. In the next stage of the experiment, PpIX analysis was performed in glioblastoma cell lines. The lines U87MG-IDH1WT harboring wild-type IDH1 and U87MG-IDH1R132H representing the mutant gene variant were used in the experiment. The authors showed a significant delay in PpIX metabolism due to the IDH mutation. In the case of U87MG-IDH1WT cells, an intense increase in fluorescence was noted as early as 1 h after incubation. In U87MG-IDH1R132H cells, the increase in fluorescence was noticeably later. In order to understand the exact nature of this relationship, the authors assessed tricarboxylic acid (TCA) cycle-related metabolite changes using LC–MS. After administration of 5-ALA, a

significant increase in the concentration of citrate and a decrease in the concentration of α-ketoglutarate (α-KG) in cells presenting the mutated gene variant were noted. A similar relationship was not observed in the U87MG-IDH1WT line. Additionally, a higher production of R-2-hydroxyglutarate (2-HG) was demonstrated in mutant cells both with and without exposure to 5-ALA. The authors also observed a decrease in baseline NADPH levels in cells bearing the IDH1 mutation compared with WT. After, exposure to 5-ALA NADPH was almost depleted in both cell lines [218]. It has therefore been hypothesized that it is the balance of this compound that may be crucial for heme metabolism and PpIX accumulation.

NADPH is involved in many metabolic chains of the organism and plays an important role in neoplastic cells in which the pathways of its transformation are often disturbed [237,238]. As mentioned before, physiologically, ALA is produced from the Krebs cycle succinyl-CoA and glycine in a reaction catalyzed by ALA synthase [45,93,190,230]. This enzyme is the natural regulatory point of heme metabolism. The excess of heme inhibits the synthase function (inhibiting endogenous ALA production) and at the same time stimulates the action of HO-1, which in the feedback mechanism enhances its degradation [230]. HO-1 breaks down heme together with NADPH reductase. It has been shown that HO-1 activity can be increased also in the presence of NADPH and NADH [239]. The presence of the IDH1/2 mutation greatly influences the availability of NADPH. Data available in the literature suggest that its primary source in human brain cells and gliomas is the pentose phosphate pathway regulated by the activity of isocitrate dehydrogenase, which catalyzes the conversion of isocitrate to α-KG [240]. The IDH1/2 mutation causes a decrease in enzyme activity, leading to impaired NADPH production. In addition, its consumption is also increasing in the pathological production of 2-HG from a-KG in the reduction process dependent on NADPH [233]. The effect may be a significant deficiency of NADPH, resulting in an insufficiently effective work of HO-1. It has been shown that in glioblastoma cells with an IDH1 mutation, the production of the compound is reduced by more than 40% [235,241]. The addition of exogenous ALA overactivates the heme metabolic pathway to break down 5-ALA excess. With concomitant NADPH deficiency, HO-1 function is limited, resulting in low FECH expression and consequently increased PpIX accumulation. It is this mechanism that likely causes the temporary increase in fluorescence in IDH-1 mutant cells demonstrated by Kim et al. [218].

The authors explored the role of NADPH in the regulation of PpIX accumulation and fluorescence with another paper in which three types of glioblastoma tissue (collected from five patients) were carefully scrutinized and characterized in terms of luminosity as strong, weak, and absent. Then, using RNA sequencing, they showed that the expression of 77 genes was directly and that of 508 genes inversely proportional to the intensity of the fluorescence. The effects of IDH mutations on protoporphyrin IX metabolism are shown in Figure 2. In the next stage of the experiment, Kim et al. examined the role of glutaminase 2 (GLS2) in the heterogeneity of the tumor tissue fluorescence [80]. Glutaminase is an enzyme that converts glutamine to glutamate and ammonium in the mitochondria [242]. Importantly, it has been proven that glutamine is the basic metabolic fuel for neoplastic cells, including glial ones [80,119,243–245]. The glutamate derived from the transformation is then converted to α-KG and incorporated into the Krebs cycle [242]. Glutaminase has two isoforms: the renal type (GLS), which is expressed in most tissues, and the hepatic type (GLS2), which is present in the brain, liver, and pancreas [246]. They differ in terms of regulating factors and their role in the oncogenesis process [235,242,244,247,248]. In glioblastoma cells, silencing of GLS induces apoptosis, while overexpression of GLS2 inhibits tumor growth [249]. An experiment by Kim et al. showed that GLS2 expression inversely correlated with the intensity of cell fluorescence. Likewise, the transfection of the GLS2 gene construct into the glioblastoma cell lines (T98G, U87MG, and LN18) resulted in a decrease in PpIX accumulation and lower glow level in the samples. It was thus confirmed that decreased GLS2 expression is associated with increased PpIX fluorescence intensity [80]. Importantly, downregulation of GLS2 has been recognized as a hallmark

of glioma cells [244,245,248,250]. Conversely, Kim et al. in their study showed that high GLS2 expression was associated with an increase in NADPH production. While exposure to 5-ALA results in a significant reduction in NADPH/NADP and reduced glutathione (GSH)/oxidized glutathione (GSSG) levels, GLS2 expression partially reverses this effect, for it is associated with an increase in NADPH/NADP levels [80]. The collected data show that cells with high GLS2 expression are characterized by a high ability to metabolize 5-ALA, while the reduction of its expression (characteristic of gliomas) may contribute to a delay in metabolism and, as a result, greater accumulation of PpIX, inducing a transient increase in cell fluorescence [80,218]. In order to confirm this relationship, Kim et al. checked the NADPH/NADP ratio in glioblastoma areas characterized by a different light intensity. It has been shown that the nonfluorescent regions show an increased NADPH/NADP ratio compared with the positive glow regions [80].

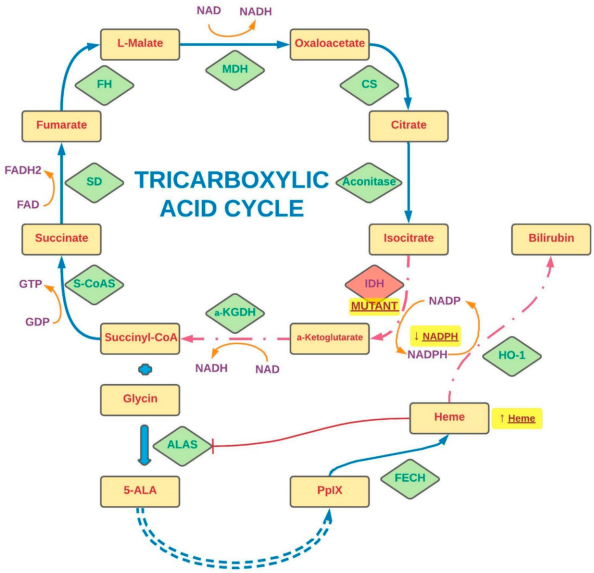

Figure 2. The stages of the tricarboxylic acid cycle and the effects of IDH mutations on protoporphyrin IX metabolism. The synthesis steps are indicated by solid arrows, and the regulatory steps by dashed arrows. The shortened conversions are marked by a double-dashed arrow. A red indicator (T) points to a transformation inhibited by another factor. The effects of IDH mutations are highlighted by a yellow glow. S-CoAS—Succinyl-CoA synthetase, SD—succinate dehydrogenase, FH—fumarase, MDH—malate dehydrogenase, CS—citrate synthase, IDH—isocitrate dehydrogenase, α-KGDH—α-ketoglutarate dehydrogenase, ALAS—ALA synthase, FECH—ferrochelatase, HO-1—heme oxygenase-1, 5-ALA—5-aminolevulinic acid, PpIX—protoporphyrin IX, NAD—nicotinamide adenine dinucleotide, NADP—nicotinamide adenine dinucleotide phosphate, GDP—guanosine diphosphate, GTP—guanosine-5′-triphosphate.

4. Effect of Accompanying Treatment on 5-Aminolevulinic Acid-Induced Fluorescence

Discrepancies between the results of in vitro studies and the actual fluorescence observed clinically during surgery might also raise suspicions of potential disturbances in PpIX metabolism induced by concomitant treatment administered to patients with gliomas. Accordingly, epileptic seizures are a very common symptom associated with intracranial tumors. It is estimated that they occur in over 40% of patients with HGG [251]. The proportion increases even more in recurrent lesions [252]. For this reason, the use of antiepileptic drugs (AEDs) is very common in this group of patients [253–255]. Standard treatment options include phenytoin (PHY), carbamazepine, valproic acid, and levetiracetam (LEV) [256–258]. Some authors have suggested that the administration of antiepileptic drugs may interfere with the PpIX accumulation and fluorescence process induced by 5-ALA administration. This relationship was demonstrated in a previously mentioned study performed on LGG by Goryaynov et al. The authors showed that among the group of patients taking antiepileptic

drugs, tumor fluorescence was seen in only 27% of cases. In comparison, for those without this form of treatment, the percentage was 83% [114]. In another study, Lawrence et al. used the glioblastoma cell line (U87MG) exposing the cells to antiepileptic drugs (phenytoin, valproic acid, and levetiracetam) as well as other substances commonly used in patients with intracranial tumors, such as steroids (dexamethasone) and antidepressants (desipramine). The results showed that for all these substances, except levetiracetam, a reduction in PpIX synthesis in GBM cells was present. What is more, combining dexamethasone with any of the drugs (including levetiracetam) resulted in an even greater reduction in a dye production. It is worth noting, however, that the supply of the steroid was associated with greater PpIX cell retention compared with the control sample. Concomitant use of dexamethasone with desipramine, valproic acid, or levetiracetam did not affect dye retention, while the combination of the steroid with phenytoin was associated with its significant reduction [259]. It has also been suggested that the supply of corticosteroids may seal off the blood–brain barrier, leading to weaker 5-ALA penetration into tumor cells and subsequently weaker PpIX fluorescence [84,260]. Interestingly, one of the first studies on intraoperative navigation using 5-ALA considered including preoperative dexamethasone in the standard operating protocol [24,261]. However, this is not a common practice at present in view of the available data. In another study, Hefti et al. analyzed the effect of phenytoin and levetiracetam on the accumulation of PpIX in glioblastoma cell lines (U373 MG and U-87 MG) and in tumor samples obtained from biopsies of patients who received 5-ALA. The authors demonstrated a dose-dependent reduction in PpIX accumulation in all cell types exposed to phenytoin. Interestingly, no similar relationship was found for levetiracetam [262]. Since the authors related this phenomenon to the disturbance of the PpIX mitochondrial synthesis, they assessed their function by measuring the mitochondrial membrane potential (MMP). Again, the study showed a reduction in mitochondrial membrane potentials only after exposure to phenytoin. At the same time, no morphological and necrotic changes or disturbances in glutathione status, being an indicator of oxidative stress, were observed for both drugs [218]. It was suggested that the changes observed were consequences of the damage to protein and lipids induced by phenytoin and its metabolites, resulting in membrane disorders [262–264]. To conclude from studies by Hefti et al. and Lawrence et al., one ought to remember that in patients operated with the use of 5-ALA for fluorescent intraoperative navigation, levetiracetam should be the preferred antiepileptic drug [259,262].

Still the exact mechanism of the influence of concomitant pharmacotherapy on PpIX metabolism remains unknown. Haust et al. in 1989 described the effects of antiepileptic drugs (carbamazepine and valproic acid) on 5-aminolevulinic acid dehydratase and uroporphyrinogen I synthetase activities in erythrocytes of a vitamin B6-deficient epileptic boy. The authors reported that long-term drug use led to decreased activities of 5-aminolevulinic acid dehydratase and uroporphyrinogen I synthetase, while increasing the concentration of erythrocyte protoporphyrin. Pb poisoning, iron depletion, and erythropoietic protoporphyria [265] were not observed. This suggests the direct influence of antiepileptic drugs on the PpIX synthesis enzymes in the mitochondria; however, a detailed understanding of this relationship requires further observations. Not all authors have agreed about the effects of AEDs and steroids on PpIX accumulation. Wadiura et al., who retrospectively analyzed the treatment of 110 glioblastoma patients (WHO II–IV) operated on with 5-ALA navigation, found that visible fluorescence was noted only in 35% of the patients. Nonetheless, the majority of the group consisted of low-grade tumors (WHO II—59%). Of all patients, 66% of the group received preoperative premedication with antiepileptic drugs. The most frequently administered drug was levetiracetam alone or in combination with substances from other groups. Analysis of the collected data showed no statistically significant correlation of the percentages of 5-ALA fluorescence between the groups of patients not taking AEDs (29%), taking LEV alone (43%), taking LEV with another AED (45%), and taking other AED (32%). Still, some of the patients enrolled in the study were also premedicated with dexamethasone (24%). In those cases, univariate analysis showed a statistically significant

difference in the percentages of tumors with positive fluorescence between patients receiving preoperative steroid therapy (54%) and those without such therapy (31%). It should be noted though that steroids were administered much more frequently in HGG, which may have biased the data to some extent. Comparison of data only for tumors with the same WHO grading did not show a statistically significant relationship in the fluorescence of tumors in patients receiving and not receiving dexamethasone (WHO II: 11% vs. 11%, WHO III/IV: 77% vs. 71% [103].

5. Conclusions

According to the data available in the literature, the use of 5-ALA in intraoperative fluorescence navigation may bring notable benefits in the surgical treatment of patients with glial tumors, resulting in a better therapeutic outcome [18,42,43]. Unfortunately, as clinical practice shows, in many cases the operated tumors differ in the level of emitted fluorescence, which often complicates the course of resection. Moreover, this phenomenon remains largely unpredictable, introducing an element of randomness to the therapy of patients. For this reason, it is important to identify factors that may enhance or disrupt the phenomenon of PpIX fluorescence in glial tumor cells exposed to 5-ALA. In the light of the reviewed publications, many authors suggest that these discrepancies may be due to the different expression and activity of enzymes involved in the metabolism of 5-ALA depending on the histopathological characteristics of the tumor. However, as some of the studies show, the different rate of cell division may also have a significant impact on the expression of particular enzymes involved in the metabolism of protoporphyrin IX, such as PBGD, FECH, UROS, and ALAS [64,66,77,78]. In addition, the dynamics of these processes depends also on the function of proteins involved in the transport of dyes and their metabolites. These include ABCB6 and ABCG2 [89,149,153]. The differences in the intensity of the emitted light between different tumors may also result from impaired penetration of the dye through the blood–brain barrier. Most researchers agree that some degree of damage to the BBB by the tumor is a necessary prerequisite for selective 5-ALA accumulation in the tumor cells. This may be one of the differences observed in the intensity of fluorescence or lack of fluorescence in different brain tumors [122,125].

The use of substances and physical methods that potentiate the emitted fluorescence may also be of great significance. Some authors have attempted to identify tumor profiles that favor fluorescence. These studies include the Ki-67/MIB-1 index, MGMT status, IDH mutation, and 1p/19q codeletion. While in the case of the Ki-67/MIB-1 index and IDH mutation data available in the literature are mostly consistent, in other cases, further observations are needed to assess their significance [19,101,106]. Moreover, the drugs used in standard therapy for patients with CNS tumors may also affect 5-ALA metabolism pathways. Some authors have suggested the importance of certain antiepileptic drugs, such as phenytoin, carbamazepine, valproic acid, and levetiracetam, in this regard [262]. This effect was potentiated by the addition of dexamethasone [259]. The mechanism underlying this relationship is still not fully understood. It can take place both through the influence of drugs on the mitochondrial membrane potential and through the influence on the activity of some enzymes, such as UROS or ALAD. This draws attention to the possibility of an appropriate treatment setting in patients for whom intraoperative fluorescence navigation is used.

Furthermore, it is worth noting that the nature of tumor cell fluorescence is a complex phenomenon. This article focuses primarily on variations resulting from different accumulations of PpIX, the main source of excited light. This is a key aspect, especially in in vitro observations, where light measurement is always performed under analogous conditions using the same instruments. However, it should be noted that the fluorescence intensity also depends on both the equipment used to induce PpIX to emit fluorescence (operating microscope, set of filters determining the light wavelength, or characteristics of the lamps used in the laboratory) and the sensitivity of the detection device. The relationship between the fluorescence intensity of PpIX and the excitation light source is described in a paper by

Kamp et al. [266,267]. Belykh et al. also conducted a detailed analysis of the light profile of clinical-grade operating microscopes used for PpIX visualization [268]. In the case of in vivo studies, photobleaching is also an issue. This phenomenon consists in a gradual reduction of the fluorescence emitted by PpIX under prolonged exposure to excitation light [18,268]. It should be mentioned that in some of the works describing intraoperative light emission in vivo in which it was impossible to use specialized measuring equipment, the assessment was made on the basis of the surgeon's judgement, which unfortunately is an imperfect tool. This highlights the problem of the difficulty in objectively assessing the intensity of emitted fluorescence. However, some authors have made efforts to develop a tool that allows more accurate and reproducible measurements [268]. The above article summarizes the currently available knowledge regarding the differences in the level of fluorescence emitted among the data available in the literature. However, in order to fully realize the potential of this therapeutic method, it is crucial to understand all the relationships governing protoporphyrin IX metabolism and their influence on fluorescence emission by tumor cells. This will allow both for increasing the effectiveness of this navigation method and for defining the optimal group of patients in whom the use of fluorescence navigation can bring maximum benefit.

Author Contributions: Conceptualization: M.M. and R.R.; methodology: M.M. and D.S.; validation: M.M., A.O., and D.S.; formal analysis: M.M. and A.O.; investigation: M.M., D.S., and A.O.; resources: M.M., D.S., and A.O.; data curation: M.M.; writing—original draft preparation: M.M.; writing—review and editing: R.R. and D.S.; visualization: M.M.; supervision: R.R. and D.S.; project administration: M.M. and R.R.; funding acquisition: R.R. and D.S. All authors have read and agreed to the published version of the manuscript.

Funding: This research received no external funding.

Institutional Review Board Statement: Not applicable.

Informed Consent Statement: Not applicable.

Data Availability Statement: Not applicable.

Conflicts of Interest: The authors declare no conflict of interest.

References

1. Allikmets, R.; Gerrard, B.; Hutchinson, A.; Dean, M. Characterization of the human ABC superfamily: Isolation and mapping of 21 new genes using the expressed sequence tags database. *Hum. Mol. Genet.* **1996**, *5*, 1649–1655. [CrossRef] [PubMed]
2. Salomon, D.S.; Brandt, R.; Ciardiello, F.; Normanno, N. Epidermal growth factor-related peptides andtheir receptors in human malignancies. *Crit. Rev. OncolHematol.* **1995**, *19*, 183–232. [CrossRef]
3. Mazurek, M.; Litak, J.; Kamieniak, P.; Kulesza, B.; Jonak, K.; Baj, J.; Grochowski, C. Metformin as Potential Therapy for High-Grade Glioma. *Cancers* **2020**, *12*, 210. [CrossRef]
4. Porter, K.R.; McCarthy, B.J.; Berbaum, M.L.; Davis, F.G. Conditional survival of all primary brain tumor patients by age, behavior, and histology. *Neuroepidemiology* **2011**, *36*, 230–239. [CrossRef] [PubMed]
5. Visser, O.; Ardanaz, E.; Botta, L.; Sant, M.; Tavilla, A.; Minicozzi, P.; EUROCARE-5 Working Group. Survival of adults with primary malignant brain tumours in Europe; Results of the EUROCARE-5 study. *Eur. J. Cancer* **2015**, *51*, 2231–2241. [CrossRef] [PubMed]
6. Aldape, K.; Brindle, K.M.; Chesler, L.; Chopra, R.; Gajjar, A.; Gilbert, M.R.; Gottardo, N.; Gutmann, D.; Hargrave, D.; Holland, E.C.; et al. Challenges to curing primary brain tumours. *Nat. Rev. Clin. Oncol.* **2019**, *16*, 509–520. [CrossRef]
7. Mazurek, M.; Grochowski, C.; Litak, J.; Osuchowska, I.; Maciejewski, R.; Kamieniak, P. Recent Trends of microRNA Significance in Pediatric Population Glioblastoma and Current Knowledge of Micro RNA Function in Glioblastoma Multiforme. *Int. J. Mol. Sci.* **2020**, *21*, 3046. [CrossRef] [PubMed]
8. Lara-Velazquez, M.; Al-Kharboosh, R.; Jeanneret, S.; Vazquez-Ramos, C.; Mahato, D.; Tavanaiepour, D.; Rahmathulla, G.; Quinones-Hinojosa, A. Advances in Brain Tumor Surgery for Glioblastoma in Adults. *Brain Sci.* **2017**, *7*, 166. [CrossRef]
9. D'Alessio, A.; Proietti, G.; Sica, G.; Scicchitano, B.M. Pathological and Molecular Features of Glioblastoma and Its Peritumoral Tissue. *Cancers* **2019**, *11*, 469. [CrossRef] [PubMed]
10. Suchorska, B.; Weller, M.; Tabatabai, G.; Senft, C.; Hau, P.; Sabel, M.C.; Herrlinger, U.; Ketter, R.; Schlegel, U.; Marosi, C.; et al. Complete resection of contrast-enhancing tumor volume is associated with improved survival in recurrent glioblastoma—Results from the DIRECTOR trial. *Neuro-Oncology* **2016**, *18*, 549–556. [CrossRef]
11. Stanescusegall, D.; Jackson, T. Vital staining with indocyanine green: A review of the clinical and experimental studies relating to safety. *Eye* **2009**, *23*, 504–518. [CrossRef]

12. Choi, M.; Chung, T.; Choi, K.; Choi, C. Dynamic fluorescence imaging for multiparametric measurement of tumor vasculature. *J. Biomed. Opt.* **2011**, *16*, 46008. [CrossRef] [PubMed]
13. Chaichana, K.L.; Chaichana, K.K.; Olivi, A.; Weingart, J.D.; Bennett, R.; Brem, H.; Quiñones-Hinojosa, A. Surgical outcomes for older patients with glioblastoma multiforme: Preoperative factors associated with decreased survival: Clinical article. *J. Neurosurg.* **2011**, *114*, 587–594. [CrossRef]
14. Velde, E.T.; Veerman, T.; Subramaniam, V.; Ruers, T. The use of fluorescent dyes and probes in surgical oncology. *Eur. J. Surg. Oncol.* **2010**, *36*, 6–15. [CrossRef] [PubMed]
15. Stummer, W.; Meinel, T.; Ewelt, C.; Martus, P.; Jakobs, O.; Felsberg, J.; Reifenberger, G. Prospective cohort study of radiotherapy with concomitant and adjuvant temozolomide chemotherapy for glioblastoma patients with no or minimal residual enhancing tumor load after surgery. *J. Neuro-Oncol.* **2012**, *108*, 89–97. [CrossRef] [PubMed]
16. Castano, A.P.; Demidova, T.N.; Hamblin, M.R. Mechanisms in photodynamic therapy: Part two—cellular signaling, cell metabolism and modes of cell death. *Photodiagn. Photodyn. Ther.* **2005**, *2*, 1–23. [CrossRef]
17. Akimoto, J. Photodynamic Therapy for Malignant Brain Tumors. *Neurol. Med.-Chir.* **2016**, *56*, 151–157. [CrossRef] [PubMed]
18. Gandhi, S.; Meybodi, A.T.; Belykh, E.; Cavallo, C.; Zhao, X.; Syed, M.P.; Moreira, L.B.; Lawton, M.T.; Nakaji, P.; Preul, M.C. Survival Outcomes among Patients With High-Grade Glioma Treated with 5-Aminolevulinic Acid–Guided Surgery: A Systematic Review and Meta-Analysis. *Front. Oncol.* **2019**, *9*, 620. [CrossRef]
19. Stummer, W.; Novotny, A.; Stepp, H.; Goetz, C.; Bise, K.; Reulen, H.J. Fluorescence-guided resection of glioblastoma multiforme by using 5-aminolevulinic acid-induced porphyrins: A prospective study in 52 consecutive patients. *J. Neurosurg.* **2000**, *93*, 1003–1013. [CrossRef]
20. Valle, R.D.; Hadjipanayis, C.G.; Stummer, W. Established and emerging uses of 5-ALA in the brain: An overview. *J. Neuro-Oncol.* **2019**, *141*, 487–494. [CrossRef]
21. Regula, J.; MacRobert, A.J.; Gorchein, A.; Buonaccorsi, G.A.; Thorpe, S.M.; Spencer, G.M.; Hatfield, A.R.; Bown, S.G. Photosensitisation and photodynamic therapy of oesophageal, duodenal, and colorectal tumours using 5 aminolaevulinic acid induced protoporphyrin IX-a pilot study. *Gut* **1995**, *36*, 67–75. [CrossRef]
22. Walter, S.; Susanne, S.; Simon, W.; Herbert, S.; Clemens, F.; Claudia, G.; Alwin, E.G.; Rainer, K.; Hans, J.R. Intraoperative detection of malignant gliomas by 5-aminolevulinic acid-induced porphyrin fluorescence. *Neurosurgery* **1998**, *42*, 518–526. [CrossRef]
23. Esteves, S.; Alves, M.; Castel-Branco, M.; Stummer, W. A pilot cost-effectiveness analysis of treatments in newly diagnosed high-grade gliomas. *Neurosurgery* **2015**, *76*, 552–562. [CrossRef] [PubMed]
24. Stummer, W.; Pichlmeier, U.; Meinel, T.; Wiestler, O.D.; Zanella, F.; Reulen, H.-J.; ALA-Glioma Study Group. Fluorescence-guided surgery with 5-aminolevulinic acid for resection of malignant glioma: A randomised controlled multicentre phase III trial. *Lancet Oncol.* **2006**, *7*, 392–401. [CrossRef]
25. Belykh, E.; Martirosyan, N.L.; Yagmurlu, K.; Miller, E.J.; Eschbacher, J.M.; Izadyyazdanabadi, M.; Bardonova, L.A.; Byvaltsev, V.; Nakaji, P.; Preul, M.C. Intraoperative Fluorescence Imaging for Personalized Brain Tumor Resection: Current State and Future Directions. *Front. Surg.* **2016**, *3*, 55. [CrossRef] [PubMed]
26. Stummer, W.; Stocker, S.; Novotny, A.; Heimann, A.; Sauer, O.; Kempski, O.; Plesnila, N.; Wietzorrek, J.; Reulen, H. In vitro and in vivo porphyrin accumulation by C6 glioma cells after exposure to 5-aminolevulinic acid. *J. Photochem. Photobiol. B Biol.* **1998**, *45*, 160–169. [CrossRef]
27. Stummer, W.; Molina, E.S. Fluorescence imaging/agents in tumor resection. *Neurosurg. Clin. N. Am.* **2017**, *28*, 569–583. [CrossRef] [PubMed]
28. Roberts, D.W.; Valdés, P.A.; Harris, B.T.; Hartov, A.; Fan, X.; Ji, S.; Leblond, F.; Tosteson, T.D.; Wilson, B.C.; Paulsen, K.D. Glioblastoma multiforme treatment with clinical trials for surgical resection (aminolevulinic acid). *Neurosurg. Clin. N. Am.* **2012**, *23*, 371–377. [CrossRef]
29. Idoate, M.A.; Valle, R.D.; Echeveste, J.; Tejada, S. Pathological characterization of the glioblastoma border as shown during surgery using 5-aminolevulinic acid-induced fluorescence. *Neuropathology* **2011**, *31*, 575–582. [CrossRef]
30. Stummer, W.; Stepp, H.; Möller, G.; Ehrhardt, A.; Leonhard, M.; Reulen, H.J. Technical principles for protoporphyrin-ix-fluorescence guided microsurgical resection of malignant glioma tissue. *Acta Neurochir.* **1998**, *140*, 995–1000. [CrossRef]
31. Coburger, J.; Engelke, J.; Scheuerle, A.; Thal, D.; Hlavac, M.; Wirtz, C.R.; König, R. Tumor detection with 5-aminolevulinic acid fluorescence and Gd-DTPA–enhanced intraoperative MRI at the border of contrast-enhancing lesions: A prospective study based on histopathological assessment. *Neurosurg. Focus* **2014**, *36*, E3. [CrossRef] [PubMed]
32. Ewelt, C.; Floeth, F.W.; Felsberg, J.; Steiger, H.J.; Sabel, M.; Langen, K.-J.; Stoffels, G.; Stummer, W. Finding the anaplastic focus in diffuse gliomas: The value of Gd-DTPA enhanced MRI, FET-PET, and intraoperative, ALA-derived tissue fluorescence. *Clin. Neurol. Neurosurg.* **2011**, *113*, 541–547. [CrossRef] [PubMed]
33. Valdés, P.A.; Kim, A.; Leblond, F.; Conde, O.M.; Harris, B.T.; Paulsen, K.D.; Wilson, B.C.; Roberts, D.W. Combined fluorescence and reflectance spectroscopy for in vivo quantification of cancer biomarkers in low- and high-grade glioma surgery. *J. Biomed. Opt.* **2011**, *16*, 116007–11600714. [CrossRef]
34. Su, X.; Huang, Q.-F.; Chen, H.-L.; Chen, J. Fluorescence-guided resection of high-grade gliomas: A systematic review and meta-analysis. *Photodiagn. Photodyn. Ther.* **2014**, *11*, 451–458. [CrossRef]
35. Panciani, P.P.; Fontanella, M.; Schatlo, B.; Garbossa, D.; Agnoletti, A.; Ducati, A.; Lanotte, M. Fluorescence and image guided resection in high grade glioma. *Clin. Neurol. Neurosurg.* **2012**, *114*, 37–41. [CrossRef] [PubMed]

36. Zhao, S.; Wu, J.; Wang, C.; Liu, H.; Dong, X.; Shi, C.; Shi, C.; Liu, Y.; Teng, L.; Han, D.; et al. Intraoperative fluorescence-guided resection of high-grade malignant gliomas using 5-aminolevulinic acid–induced porphyrins: A systematic review and meta-analysis of prospective studies. *PLoS ONE* **2013**, *8*, e63682. [CrossRef] [PubMed]
37. Hefti, M.; Von Campe, G.; Moschopulos, M.; Siegner, A.; Looser, H.; Landolt, H. 5-aminolevulinic acid induced protoporphyrin IX fluorescence in high-grade glioma surgery: A one-year experience at a single institutuion. *Swiss. Med. Wkly.* **2008**, *138*, 180–185. [PubMed]
38. Valdés, P.A.; Leblond, F.; Kim, A.; Harris, B.T.; Wilson, B.C.; Fan, X.; Tosteson, T.D.; Hartov, A.; Ji, S.; Erkmen, K.; et al. Quantitative fluorescence in intracranial tumor: Implications for ALA-induced PpIX as an intraoperative biomarker. *J. Neurosurg.* **2011**, *115*, 11–17. [CrossRef] [PubMed]
39. Floeth, F.W.; Sabel, M.; Ewelt, C.; Stummer, W.; Felsberg, J.; Reifenberger, G.; Steiger, H.J.; Stoffels, G.; Coenen, H.H.; Langen, K.-J. Comparison of 18F-FET PET and 5-ALA fluorescence in cerebral gliomas. *Eur. J. Nucl. Med. Mol. Imaging* **2010**, *38*, 731–741. [CrossRef]
40. Kremer, P.; Fardanesh, M.; Ding, R.; Pritsch, M.; Zoubaa, S.; Frei, E. Intraoperative fluorescence staining of malignant brain tumors using 5-aminofluorescein-labeled albumin. *Oper. Neurosurg.* **2009**, *64* (Suppl. 3), ONS53–ONS60, discussion ONS60–ONS61. [CrossRef]
41. Valle, R.D.; Slof, J.; Galván, J.; Arza, C.; Romariz, C.; Vidal, C.; VISIONA Study Researchers. Observational, retrospective study of the effectiveness of 5-aminolevulinic acid in malignant glioma surgery in Spain (The VISIONA study). *Neurologia* **2014**, *29*, 131–138. [CrossRef]
42. Diez-Valle, R.; Tejada-Solis, S.; Idoate-Gastearena, M.; Garcia-De-Eulate, R.; Dominguez, P.D.; Mendiroz, J.A. Surgery guided by 5-aminolevulinic fluorescence in glioblastoma: Volumetric analysis of extent of resection in single-center experience. *J. Neuro-Oncol.* **2011**, *102*, 105–113. [CrossRef] [PubMed]
43. Della Puppa, A.; Ciccarino, P.; Lombardi, G.; Rolma, G.; Cecchin, D.; Rossetto, M. 5-Aminolevulinic acid fluorescence in high grade glioma surgery: Surgical outcome, intraoperative findings, and fluorescence patterns. *BioMed Res. Int.* **2014**, *2014*, 232561. [PubMed]
44. Gan, H.K.; Cvrljevic, A.N.; Johns, T.G. The epidermal growth factor receptor variant III (EGFRvIII): Where wild things are altered. *FEBS J.* **2013**, *280*, 5350–5370. [CrossRef] [PubMed]
45. Ishizuka, M.; Abe, F.; Sano, Y.; Takahashi, K.; Inoue, K.; Nakajima, M.; Kohda, T.; Komatsu, N.; Ogura, S.-I.; Tanaka, T. Novel development of 5-aminolevurinic acid (ALA) in cancer diagnoses and therapy. *Int. Immunopharmacol.* **2011**, *11*, 358–365. [CrossRef]
46. Piffaretti, D.; Burgio, F.; Thelen, M.; Kaelin-Lang, A.; Paganetti, P.; Reinert, M.; D'Angelo, M.L. Protoporphyrin IX tracer fluorescence modulation for improved brain tumor cell lines visualization. *J. Photochem. Photobiol. B Biol.* **2019**, *201*, 111640. [CrossRef]
47. Scotto, A.W.; Chang, L.F.; Beattie, D.S. The characterization and submitochondrial localization of delta-aminolevulinic acid synthase and an associated amidase in rat liver mitochondria using an improved assay for both enzymes. *J. Biol. Chem.* **1983**, *258*, 81–90. [CrossRef]
48. Yang, X.; Palasuberniam, P.; Kraus, D.; Chen, B. Aminolevulinic Acid-Based Tumor Detection and Therapy: Molecular Mechanisms and Strategies for Enhancement. *Int. J. Mol. Sci.* **2015**, *16*, 25865–25880. [CrossRef]
49. May, B.K.; Bawden, M.J. Control of heme biosynthesis in animals. *Semin. Hematol.* **1989**, *26*, 150–156.
50. Ponka, P. Cell biology of heme. *Am. J. Med Sci.* **1999**, *318*, 241–256. [CrossRef]
51. Moore, M.R.; McColl, K.E.L.; Rimington, C.; Goldberg, A. *Disorders of Porphyrin Metabolism*; Plenum Press: New York, NY, USA, 1987.
52. Grandchamp, B.; Phung, N.; Nordmann, Y. The mitochondrial localization of coproporphyrinogen III oxidase. *Biochem. J.* **1978**, *176*, 97–102. [CrossRef]
53. Teng, L.; Nakada, M.; Hayashi, Y.; Yoneyama, T.; Zhao, S.-G.; Hamada, S.-G.Z.A.J.-I. Current Applications of 5-ALA in Glioma Diagnostics and Therapy. In *Clinical Management and Evolving Novel Therapeutic Strategies for Patients with Brain Tumors*; Terry Lichtor, IntechOpen, 2013; Available online: https://www.intechopen.com/chapters/43910 (accessed on 15 November 2021).
54. Ferreira, G.C.; Andrew, T.L.; Karr, S.W.; Dailey, H.A. Organization of the terminal two enzymes of the heme biosynthetic pathway. Orientation of protoporphyrinogen oxidase and evidence for a membrane complex. *J. Biol. Chem.* **1988**, *263*, 3835–3839. [CrossRef]
55. Ferraro, N.; Barbarite, E.; Albert, T.R.; Berchmans, E.; Shah, A.H.; Bregy, A.; Ivan, M.E.; Brown, T.; Komotar, R.J. The role of 5-aminolevulinic acid in brain tumor surgery: A systematic review. *Neurosurg. Rev.* **2016**, *39*, 545–555. [CrossRef]
56. Elder, G.H.; Evans, J.O. Evidence that the coproporphyrinogen oxidase activity of rat liver is situated in the intermembrane space of mitochondria. *Biochem. J.* **1978**, *172*, 345–347. [CrossRef] [PubMed]
57. Fontana, A.O.; Piffaretti, D.; Marchi, F.; Burgio, F.; Faia-Torres, A.B.; Paganetti, P.; Pinton, S.; Pieles, U.; Reinert, M. Epithelial growth factor receptor expression influences 5-ALA induced glioblastoma fluorescence. *J. Neuro-Oncol.* **2017**, *133*, 497–507. [CrossRef] [PubMed]
58. Khan, A.A.; Quigley, J.G. Control of intracellular heme levels: Heme transporters and heme oxygenases. *Biochim. Biophys. Acta* **2011**, *1813*, 668–682. [CrossRef]
59. Hagiya, Y.; Endo, Y.; Yonemura, Y.; Takahashi, K.; Ishizuka, M.; Abe, F.; Tanaka, T.; Okura, I.; Nakajima, M.; Ishikawa, T.; et al. Pivotal roles of peptide transporter PEPT1 and ATP-binding cassette (ABC) transporter ABCG2 in 5-aminolevulinic acid (ALA)-based photocytotoxicity of gastric cancer cells in vitro. *Photodiagn. Photodyn. Ther.* **2012**, *9*, 204–214. [CrossRef] [PubMed]
60. Robey, R.W.; Steadman, K.; Polgar, O.; Bates, S.E. ABCG2-mediated transport of photosensitizers: Potential impact on photodynamic therapy. *Cancer Biol. Ther.* **2005**, *4*, 187–194. [CrossRef] [PubMed]

61. Kobuchi, H.; Moriya, K.; Ogino, T.; Fujita, H.; Inoue, K.; Shuin, T.; Yasuda, T.; Utsumi, K.; Utsumi, T. Mitochondrial localization of ABC transporter ABCG2 and its function in 5-aminolevulinic acid-mediated protoporphyrin IX accumulation. *PLoS ONE* **2012**, *7*, e50082. [CrossRef] [PubMed]
62. Peng, Q.; Warloe, T.; Berg, K.; Moan, J.; Kongshaug, M.; Giercksky, K.E.; Nesland, J.M. 5-Aminolevulinic acid-based photodynamic therapy. Clinical research and future challenges. *Cancer* **1997**, *79*, 2282–2308. [CrossRef]
63. Ogino, T.; Kobuchi, H.; Munetomo, K.; Fujita, H.; Yamamoto, M.; Utsumi, T.; Inoue, K.; Shuin, T.; Sasaki, J.; Inoue, M.; et al. Serum-dependent export of protoporphyrin IX by ATP-binding cassette transporter G2 in T24 cells. *Mol. Cell. Biochem.* **2011**, *358*, 297–307. [CrossRef] [PubMed]
64. Krieg, R.C.; Messmann, H.; Rauch, J.; Seeger, S.; Knuechel, R. Metabolic characterization of tumor cell-specific protoporphyrin IX accumulation after exposure to 5-aminolevulinic acid in human colonic cells. *Photochem. Photobiol.* **2002**, *76*, 518–525. [CrossRef]
65. Mamet, R.; Leibovici, L.; Teitz, Y.; Schoenfeld, N. Accelerated heme synthesis and degradation in transformed fibroblasts. *Biochem. Med. Metab. Biol.* **1990**, *44*, 175–180. [CrossRef]
66. Greenbaum, L.; Gozlan, Y.; Schwartz, D.; Katcoff, D.J.; Malik, Z. Nuclear distribution of porphobilinogen deaminase (PBGD) in glioma cells: A regulatory role in cancer transformation? *Br. J. Cancer* **2002**, *86*, 1006–1011. [CrossRef]
67. Schoenfeld, N.; Mamet, R.; Leibovici, L.; Epstein, O.; Teitz, Y.; Atsmon, A. Growth rate determines activity of porphobilinogen deaminase both in nonmalignant and malignant cell lines. *Biochem. Med. Metab. Biol.* **1988**, *40*, 213–217. [CrossRef]
68. Hinnen, P.; de Rooij, F.W.M.; Terlouw, E.M.; Edixhoven, A.; Van Dekken, H.; Van Hillegersberg, R.; Tilanus, H.W.; Wilson, J.H.P.; Siersema, P.D. Porphyrin biosynthesis in human Barrett's oesophagus and adenocarcinoma after ingestion of 5-aminolaevulinic acid. *Br. J. Cancer* **2000**, *83*, 539–543. [CrossRef] [PubMed]
69. Gonçalves, T.L.; Erthal, F.; Corte, C.L.; Müller, L.G.; Piovezan, C.M.; Nogueira, C.W.; Rocha, J.B. Involvement of oxidative stress in the pre-malignant and malignant states of cervical cancer in women. *Clin. Biochem.* **2005**, *38*, 1071–1075. [CrossRef] [PubMed]
70. Neslund-Dudas, C.; Levin, A.M.; Rundle, A.; Beebe-Dimmer, J.; Bock, C.H.; Nock, N.L.; Jankowski, M.; Datta, I.; Krajenta, R.; Dou, Q.P.; et al. Case-only gene-environment interaction between ALAD tagSNPs and occupational lead exposure in prostate cancer. *Prostate* **2014**, *74*, 637–646. [CrossRef] [PubMed]
71. Hinnen, P.; De Rooij, F.; van Velthuysen, M.-L.; Edixhoven, A.; Van Hillegersberg, R.; Tilanus, H.; Wilson, J.; Siersema, P. Biochemical basis of 5-aminolaevulinic acid-induced protoporphyrin IX accumulation: A study in patients with (pre)malignant lesions of the oesophagus. *Br. J. Cancer* **1998**, *78*, 679–682. [CrossRef]
72. Krieg, R.C.; Fickweiler, S.; Wolfbeis, O.S.; Knuechel, R. Cell-type specific protoporphyrin IX metabolism in human bladder cancer in vitro. *Photochem. Photobiol.* **2000**, *72*, 226–233. [CrossRef]
73. Navone, N.M.; Polo, C.F.; Frisardi, A.L.; Andrade, N.E. Heme biosynthesis in human breast cancer—Mimetic "in vitro" studies and some heme enzymic activity levels. *J. Biochem.* **1990**, *22*, 1407–1411. [CrossRef]
74. Schauder, A.; Feuerstein, T.; Malik, Z. The centrality of PBGD expression levels on ALA-PDT efficacy. *Photochem. Photobiol. Sci.* **2011**, *10*, 1310–1317. [CrossRef] [PubMed]
75. Gibson, S.; Cupriks, D.; Havens, J.; Nguyen, M.; Hilf, R. A regulatory role for porphobilinogen deaminase (PBGD) in δ-aminolaevulinic acid (δ-ALA)-induced photosensitization? *Br. J. Cancer* **1998**, *77*, 235–242. [CrossRef] [PubMed]
76. Hilf, R.; Havens, J.J.; Gibson, S.L. Effect of delta-aminolevulinic acid on protoporphyrin IX accumulation in tumor cells transfected with plasmids containing porphobilinogen deaminase DNA. *Photochem. Photobiol.* **1999**, *70*, 334–340. [PubMed]
77. Ito, E.; Yue, S.; Moriyama, E.H.; Hui, A.B.; Kim, I.; Shi, W.; Alajez, N.M.; Bhogal, N.; Li, G.; Datti, A.; et al. Uroporphyrinogen decarboxylase is a radiosensitizing target for head and neck cancer. *Sci. Transl. Med.* **2011**, *3*, 67ra7. [CrossRef] [PubMed]
78. Kemmner, W.; Wan, K.; Rüttinger, S.; Ebert, B.; Macdonald, R.; Klamm, U.; Moesta, K.T. Silencing of human ferrochelatase causes abundant protoporphyrin-IX accumulation in colon cancer. *FASEB J.* **2008**, *22*, 500–509. [CrossRef]
79. Dailey, H.A.; Smith, A. Differential interaction of porphyrins used in photoradiation therapy with ferrochelatase. *Biochem. J.* **1984**, *223*, 441–445. [CrossRef]
80. Kim, S.; Kim, J.E.; Kim, Y.H.; Hwang, T.; Kim, S.K.; Xu, W.J.; Shin, J.-Y.; Kim, J.-I.; Choi, H.; Kim, H.C.; et al. Glutaminase 2 expression is associated with regional heterogeneity of 5-aminolevulinic acid fluorescence in glioblastoma. *Sci. Rep.* **2017**, *7*, 12221. [CrossRef]
81. Utsuki, S.; Oka, H.; Fujii, K. Intraoperative Photodynamic Diagnosis of Brain Tumors Using 5-Aminolevulinic Acid. In *Diagnostic Techniques and Surgical Management of Brain Tumors*; Abujamra, A.L., Ed.; InTech: Rijeka, Croatia, 2011; pp. 227–244. [CrossRef]
82. Ohgari, Y.; Nakayasu, Y.; Kitajima, S.; Sawamoto, M.; Mori, H.; Shimokawa, O.; Matsui, H.; Taketani, S. Mechanisms involved in δ-aminolevulinic acid (ALA)-induced photosensitivity of tumor cells: Relation of ferrochelatase and uptake of ALA to the accumulation of protoporphyrin. *Biochem. Pharmacol.* **2005**, *71*, 42–49. [CrossRef] [PubMed]
83. Peng, Q.; Berg, K.; Moan, J.; Kongshaug, M.; Nesland, J.M. 5-Aminolevulinic acid-based photodynamic therapy: Principles and experimental research. *Photochem. Photobiol.* **1997**, *65*, 235–251. [CrossRef]
84. Teng, L.; Nakada, M.; Zhao, S.-G.; Endo, Y.; Furuyama, N.; Nambu, E.; Pyko, I.; Hayashi, Y.; Hamada, J.-I. Silencing of ferrochelatase enhances 5-aminolevulinic acid-based fluorescence and photodynamic therapy efficacy. *Br. J. Cancer* **2011**, *104*, 798–807. [CrossRef] [PubMed]
85. Hooda, J.; Cadinu, D.; Alam, M.; Shah, A.; Cao, T.M.; Sullivan, L.A.; Brekken, R.; Zhang, L. Enhanced heme function and mitochondrial respiration promote the progression of lung cancer cells. *PLoS ONE* **2013**, *8*, e63402. [CrossRef]

86. Ishikawa, T.; Nakagawa, H. ABC transporter ABCG2 in cancer chemotherapy and pharmacogenomics. *J. Exp. Ther. Oncol.* **2009**, *8*, 5–24. [PubMed]
87. Bleau, A.-M.; Huse, J.T.; Holland, E.C. The ABCG2 resistance network of glioblastoma. *Cell Cycle* **2009**, *8*, 2937–2945. [CrossRef]
88. Jin, Y.; Bin, Z.Q.; Qiang, H.; Liang, C.; Hua, C.; Jun, D.; Dong, W.A.; Qing, L. ABCG2 is related with the grade of glioma and resistance to mitoxantone, a chemotherapeutic drug for glioma. *J. Cancer Res. Clin. Oncol.* **2009**, *135*, 1369–1376. [CrossRef] [PubMed]
89. Zhao, S.-G.; Chen, X.-F.; Wang, L.-G.; Yang, G.; Han, D.-Y.; Teng, L.; Yang, M.-C.; Wang, D.-Y.; Shi, C.; Liu, Y.-H.; et al. Increased expression of ABCB6 enhances protoporphyrin IX accumulation and photodynamic effect in human glioma. *Ann. Surg. Oncol.* **2012**, *20*, 4379–4388. [CrossRef]
90. Paterson, J.K.; Shukla, S.; Black, C.M.; Tachiwada, T.; Garfield, S.; Wincovitch, S.; Ernst, D.N.; Agadir, A.; Li, X.; Ambudkar, S.V.; et al. Human ABCB6 localizes to both the outer mitochondrial membrane and the plasma membrane. *Biochemistry* **2007**, *46*, 9443–9452. [CrossRef]
91. Matsumoto, K.; Hagiya, Y.; Endo, Y.; Nakajima, M.; Ishizuka, M.; Tanaka, T.; Ogura, S.-I. Effects of plasma membrane ABCB6 on 5-aminolevulinic acid (ALA)-induced porphyrin accumulation in vitro: Tumor cell response to hypoxia. *Photodiagn. Photodyn. Ther.* **2015**, *12*, 45–51. [CrossRef]
92. Tsuchida, M.; Emi, Y.; Kida, Y.; Sakaguchi, M. Human ABC transporter isoform B6 (ABCB6) localizes primarily in the Golgi apparatus. *Biochem. Biophys. Res. Commun.* **2008**, *369*, 369–375. [CrossRef]
93. Colditz, M.J.; van Leyen, K.; Jeffree, R.L. Aminolevulinic acid (ALA)–protoporphyrin IX fluorescence guided tumour resection. Part 2: Theoretical, biochemical and practical aspects. *J. Clin. Neurosci.* **2012**, *19*, 1611–1616. [CrossRef] [PubMed]
94. Bottomley, S.S.; Muller-Eberhard, U. Pathophysiology of heme synthesis. *Semin. Hematol.* **1988**, *25*, 282–302. [PubMed]
95. Rossi, E.; Attwood, P.V.; Garcia-Webb, P.; Costin, K.A. Inhibition of human lymphocyte ferrochelatase activity by hemin. *Biochim. Biophys. Acta* **1990**, *1038*, 375–381. [CrossRef]
96. Mazurek, M.; Kulesza, B.; Stoma, F.; Osuchowski, J.; Mańdziuk, S.; Rola, R. Characteristics of Fluorescent Intraoperative Dyes Helpful in Gross Total Resection of High-Grade Gliomas—A Systematic Review. *Diagnostics* **2020**, *10*, 1100. [CrossRef]
97. Della Puppa, A.; Lombardi, G.; Rossetto, M.; Rustemi, O.; Berti, F.; Cecchin, D.; Gardiman, M.P.; Rolma, G.; Persano, L.; Zagonel, V.; et al. Outcome of patients affected by newly diagnosed glioblastoma undergoing surgery assisted by 5-aminolevulinic acid guided resection followed by BCNU wafers implantation: A 3-year follow-up. *J. Neuro-Oncol.* **2017**, *131*, 331–340. [CrossRef]
98. Tejada-Solís, S.; Aldave-Orzaiz, G.; Pay-Valverde, E.; Marigil-Sánchez, M.; Idoate-Gastearena, M.A.; Díez-Valle, R. Prognostic value of ventricular wall fluorescence during 5-aminolevulinic-guided surgery for glioblastoma. *Acta Neurochir.* **2012**, *154*, 1997–2002, discussion 2002. [CrossRef]
99. Schucht, P.; Beck, J.; Abu-Isa, J.; Andereggen, L.; Murek, M.; Seidel, K.; Stieglitz, L.; Raabe, A. Gross total resection rates in contemporary glioblastoma surgery. *Neurosurgery* **2012**, *71*, 927–935, discussion 935–936. [CrossRef] [PubMed]
100. Ishihara, R.; Katayama, Y.; Watanabe, T.; Yoshino, A.; Fukushima, T.; Sakatani, K. Quantitative spectroscopic analysis of 5-aminolevulinic acid-induced protoporphyrin IX fluorescence intensity in diffusely infiltrating astrocytomas. *Neurol. Med.-Chir.* **2007**, *47*, 53–57, discussion 57. [CrossRef]
101. Widhalm, G.; Wolfsberger, S.; Minchev, G.; Woehrer, A.; Krssak, M.; Czech, T.; Prayer, D.; Asenbaum, S.; Hainfellner, J.A.; Knosp, E. 5-Aminolevulinic acid is a promising marker for detection of anaplastic foci in diffusely infiltrating gliomas with nonsignificant contrast enhancement. *Cancer* **2010**, *116*, 1545–1552. [CrossRef] [PubMed]
102. Widhalm, G.; Kiesel, B.; Woehrer, A.; Traub-Weidinger, T.; Preusser, M.; Marosi, C.; Prayer, D.; Hainfellner, J.A.; Knosp, E.; Wolfsberger, S. 5-Aminolevulinic Acid Induced Fluorescence Is a Powerful Intraoperative Marker for Precise Histopathological Grading of Gliomas with Non-Significant Contrast-Enhancement. *PLoS ONE* **2013**, *8*, e76988. [CrossRef] [PubMed]
103. Wadiura, L.I.; Mischkulnig, M.; Hosmann, A.; Borkovec, M.; Kiesel, B.; Rötzer, T.; Mercea, P.A.; Furtner, J.; Hervey-Jumper, S.; Rössler, K.; et al. Influence of Corticosteroids and Antiepileptic Drugs on Visible 5-Aminolevulinic Acid Fluorescence in a Series of Initially Suspected Low-Grade Gliomas Including World Health Organization Grade II, III, and IV Gliomas. *World Neurosurg.* **2020**, *137*, e437–e446. [CrossRef]
104. Jaber, M.; Wölfer, J.; Ewelt, C.; Holling, M.; Hasselblatt, M.; Niederstadt, T.; Zoubi, T.; Weckesser, M.; Stummer, W. The Value of 5-Aminolevulinic Acid in Low-grade Gliomas and High-grade Gliomas Lacking Glioblastoma Imaging Features: An Analysis Based on Fluorescence, Magnetic Resonance Imaging, 18F-Fluoroethyl Tyrosine Positron Emission Tomography, and Tumor Molecular. *Neurosurgery* **2015**, *78*, 401–411. [CrossRef]
105. Zhang, C.; Boop, F.A.; Ruge, J. The use of 5-aminolevulinic acid in resection of pediatric brain tumors: A critical review. *J. Neuro-Oncol.* **2019**, *141*, 567–573. [CrossRef] [PubMed]
106. Ohba, S.; Murayama, K.; Kuwahara, K.; Pareira, E.S.; Nakae, S.; Nishiyama, Y.; Adachi, K.; Yamada, S.; Sasaki, H.; Yamamoto, N.; et al. The Correlation of Fluorescence of Protoporphyrinogen IX and Status of Isocitrate Dehydrogenase in Gliomas. *Neurosurgery* **2020**, *87*, 408–417. [CrossRef] [PubMed]
107. McGirt, M.J.; Chaichana, K.L.; Attenello, F.J.; Weingart, J.D.; Than, K.; Burger, P.C.; Olivi, A.; Brem, H.; Quinoñes-Hinojosa, A. Extent of surgical resection is independently associated with survival in patients with hemispheric infiltrating low-grade gliomas. *Neurosurgery* **2008**, *63*, 700–708. [CrossRef] [PubMed]
108. Marbacher, S.; Klinger, E.; Schwyzer, L.; Fischer, I.; Nevzati, E.; Diepers, M.; Roelcke, U.; Fathi, A.-R.; Coluccia, D.; Fandino, J. Use of fluorescence to guide resection or biopsy of primary brain tumors and brain metastases. *Neurosurg. Focus* **2014**, *36*, E10. [CrossRef] [PubMed]

109. Saito, K.; Hirai, T.; Takeshima, H.; Kadota, Y.; Yamashita, S.; Ivanova, A.; Yokogami, K. Genetic factors affecting intraoperative 5-aminolevulinic acid-induced fluorescence of diffuse gliomas. *Radiol. Oncol.* **2017**, *51*, 142–150. [CrossRef] [PubMed]
110. Widhalm, G.; Olson, J.; Weller, J.; Bravo, J.; Han, S.J.; Phillips, J.; Hervey-Jumper, S.L.; Chang, S.M.; Roberts, D.W.; Berger, M.S. The value of visible 5-ALA fluorescence and quantitative protoporphyrin IX analysis for improved surgery of suspected low-grade gliomas. *J. Neurosurg.* **2019**, *133*, 79–88. [CrossRef] [PubMed]
111. Stockhammer, F.; Misch, M.; Horn, P.; Koch, A.; Fonyuy, N.; Plotkin, M. Association of F18-fluoro-ethyl-tyrosin uptake and 5-aminolevulinic acid-induced fluorescence in gliomas. *Acta Neurochir.* **2009**, *151*, 1377–1383. [CrossRef]
112. Ruge, J.R.; Liu, J. Use of 5-aminolevulinic acid for visualization and resection of a benign pediatric brain tumor. *J. Neurosurg. Pediatr.* **2009**, *4*, 484–486. [CrossRef]
113. Valdés, P.A.; Jacobs, V.L.; Harris, B.T.; Wilson, B.C.; Leblond, F.; Paulsen, K.D.; Roberts, D.W. Quantitative fluorescence using 5-aminolevulinic acid-induced protoporphyrin IX biomarker as a surgical adjunct in low-grade glioma surgery. *J. Neurosurg.* **2015**, *123*, 771–780. [CrossRef]
114. Goryaynov, S.; Widhalm, G.; Goldberg, M.F.; Chelushkin, D.; Spallone, A.; Chernyshov, K.A.; Ryzhova, M.; Pavlova, G.; Revischin, A.; Shishkina, L.; et al. The Role of 5-ALA in Low-Grade Gliomas and the Influence of Antiepileptic Drugs on Intraoperative Fluorescence. *Front. Oncol.* **2019**, *9*, 423. [CrossRef]
115. Kiesel, B.; Millesi, M.; Woehrer, A.; Furtner, J.; Bavand, A.; Roetzer, T.; Mischkulnig, M.; Wolfsberger, S.; Preusser, M.; Knosp, E.; et al. 5-ALA–induced fluorescence as a marker for diagnostic tissue in stereotactic biopsies of intracranial lymphomas: Experience in 41 patients. *Neurosurg. Focus* **2018**, *44*, E7. [CrossRef] [PubMed]
116. Hauser, S.B.; Kockro, R.A.; Actor, B.; Sarnthein, J.; Bernays, R.-L. Combining 5-Aminolevulinic Acid Fluorescence and Intraoperative Magnetic Resonance Imaging in Glioblastoma Surgery: A Histology-Based Evaluation. *Neurosurgery* **2015**, *78*, 475–483. [CrossRef]
117. Bruno, S.; Darzynkiewicz, Z. Cell cycle dependent expression and stability of the nuclear protein detected by Ki-67 antibody in HL-60 cells. *Cell Prolif.* **1992**, *25*, 31–40. [CrossRef]
118. Stummer, W.; Tonn, J.-C.; Goetz, C.; Ullrich, W.; Stepp, H.; Bink, A.; Pietsch, T.; Pichlmeier, U. 5-Aminolevulinic acid-derived tumor fluorescence: The diagnostic accuracy of visible fluorescence qualities as corroborated by spectrometry and histology and postoperative imaging. *Neurosurgery* **2014**, *74*, 310–319, discussion 319–320. [CrossRef]
119. Krall, A.S.; Christofk, H. Rethinking glutamine addiction. *Nat. Cell Biol.* **2015**, *17*, 1515–1517. [CrossRef]
120. Belykh, E.; Shaffer, K.V.; Lin, C.; Byvaltsev, V.A.; Preul, M.C.; Chen, L. Blood-Brain Barrier, Blood-Brain Tumor Barrier, and Fluorescence-Guided Neurosurgical Oncology: Delivering Optical Labels to Brain Tumors. *Front. Oncol.* **2020**, *10*, 739. [CrossRef] [PubMed]
121. Laiwah, A.C.Y.; Goldberg, A.; Moore, M.R. Pathogenesis and treatment of acute intermittent porphyria: Discussion paper. *J. R. Soc. Med.* **1983**, *76*, 386–392. [CrossRef] [PubMed]
122. Terr, L.; Weiner, L. An autoradiographic study of δ-aminolevulinic acid uptake by mouse brain. *Exp. Neurol.* **1983**, *79*, 564–568. [CrossRef]
123. Pallud, J.; Capelle, L.; Taillandier, L.; Fontaine, D.; Mandonnet, E.; Guillevin, R.; Bauchet, L.; Peruzzi, P.; Laigle-Donadey, F.; Kujas, M.; et al. Prognostic significance of imaging contrast enhancement for WHO grade II gliomas. *Neuro-Oncology* **2009**, *11*, 176–182. [CrossRef] [PubMed]
124. McGillion, F.; Thompson, G.; Moore, M.; Goldberg, A. The passage of δ-aminolaevulinic acid across the blood brain barrier of the rat: Effect of ethanol. *Biochem. Pharmacol.* **1974**, *23*, 472–474. [CrossRef]
125. Garcıía, S.C.; Moretti, M.B.; Garay, M.V.R.; Batlle, A. δ-Aminolevulinic acid transport through blood–brain barrier. *Gen. Pharmacol.* **1998**, *31*, 579–582. [CrossRef]
126. Louis, D.N.; Ohgaki, H.; Wiestler, O.D.; Cavenee, W.K.; Burger, P.C.; Jouvet, A.; Scheithauer, B.W.; Kleihues, P. The 2007 WHO classification of tumours of the central nervous system. *Acta Neuropathol.* **2007**, *114*, 97–109. [CrossRef] [PubMed]
127. Novotny, A.; Xiang, J.; Stummer, W.; Teuscher, N.S.; Smith, D.E.; Keep, R.F. Mechanisms of 5-Aminolevulinic acid uptake at the choroid plexus. *J. Neurochem.* **2000**, *75*, 321–328. [CrossRef] [PubMed]
128. Ennis, S.; Novotny, A.; Xiang, J.; Shakui, P.; Masada, T.; Stummer, W.; Smith, D.; Keep, R. Transport of 5-aminolevulinic acid between blood and brain. *Brain Res.* **2003**, *959*, 226–234. [CrossRef]
129. Becker, D.M.; Kramer, S.; Viljoen, J.D. Delta-aminolevulinic acid uptake by rabbit brain cerebral cortex. *J. Neurochem.* **1974**, *23*, 1019–1023. [CrossRef]
130. Cheeks, C.; Wedeen, R.P. Renal tubular transport of delta-aminolevulinic acid in rat. *Proc. Soc. Exp. Biol. Med.* **1986**, *181*, 596–601. [CrossRef]
131. Döring, F.; Walter, J.; Will, J.; Föcking, M.; Boll, M.; Amasheh, S.; Clauss, W.; Daniel, H. Delta-aminolevulinic acid transport by intestinal and renal peptide transporters and its physiological and clinical implications. *J. Clin. Investig.* **1998**, *101*, 2761–2767. [CrossRef]
132. McLoughlin, J.; Cantrill, R. The effect of delta-aminolaevulinic acid on the high affinity uptake of aspartic acid by rat brain synaptosomes. *Gen. Pharmacol.* **1984**, *15*, 553–555. [CrossRef]
133. Nir, I.; Levanon, D.; Iosilevsky, G. Permeability of blood vessels in experimental gliomas: Uptake of 99mTc-glucoheptonate and alteration in blood-brain barrier as determined by cytochemistry and electron microscopy. *Neurosurgery* **1989**, *25*, 523–531. [CrossRef]

134. Nduom, E.; Yang, C.; Merrill, M.J.; Zhuang, Z.; Lonser, R.R. Characterization of the blood-brain barrier of metastatic and primary malignant neoplasms. *J. Neurosurg.* **2013**, *119*, 427–433. [CrossRef]
135. Wesseling, P.; Van Der Laak, J.A.W.M.; De Leeuw, H.; Ruiter, D.J.; Burger, P.C. Quantitative immunohistological analysis of the microvasculature in untreated human glioblastoma multiforme. Computer-assisted image analysis of whole-tumor sections. *J. Neurosurg.* **1994**, *81*, 902–909. [CrossRef]
136. Dhermain, F.G.; Hau, P.; Lanfermann, H.; Jacobs, A.H.; van den Bent, M.J. Advanced MRI and PET imaging for assessment of treatment response in patients with gliomas. *Lancet Neurol.* **2010**, *9*, 906–920. [CrossRef]
137. Machein, M.R.; Kullmer, J.; Fiebich, B.L.; Plate, K.H.; Warnke, P.C. Vascular endothelial growth factor expression, vascular volume, and, capillary permeability in human brain tumors. *Neurosurgery* **1999**, *44*, 732–740, discussion 740-1. [CrossRef]
138. Watkins, S.; Robel, S.; Kimbrough, I.F.; Robert, S.M.; Ellisdavies, G.C.R.; Sontheimer, H. Disruption of astrocyte–vascular coupling and the blood–brain barrier by invading glioma cells. *Nat. Commun.* **2014**, *5*, 4196. [CrossRef] [PubMed]
139. Stewart, D.J. A critique of the role of the blood-brain barrier in the chemotherapy of human brain tumors. *J. Neuro-Oncol.* **1994**, *20*, 121–139. [CrossRef] [PubMed]
140. Krishnamurthy, P.; Ross, D.D.; Nakanishi, T.; Bailey-Dell, K.; Zhou, S.; Mercer, K.E.; Sarkadi, B.; Sorrentino, B.P.; Schuetz, J.D. The stem cell marker bcrp/abcg2 enhances hypoxic cell survival through interactions with heme. *J. Biol. Chem.* **2004**, *279*, 24218–24225. [CrossRef]
141. Doyle, L.A.; Yang, W.; Abruzzo, L.V.; Krogmann, T.; Gao, Y.; Rishi, A.K.; Ross, D.D. A multidrug resistance transporter from human MCF-7 breast cancer cells. *Proc. Natl. Acad. Sci. USA* **1998**, *95*, 15665–15670. [CrossRef]
142. Wakabayashi, K.; Nakagawa, H.; Adachi, T.; Kii, I.; Kobatake, E.; Kudo, A.; Ishikawa, T. Identification of cysteine residues critically involved in homodimer formation and protein expression of human ATP-binding cassette transporter ABCG2: A new approach using the flp recombinase system. *J. Exp. Ther. Oncol.* **2006**, *5*, 205–222.
143. Bart, J.; Hollema, H.; Groen, H.J.; de Vries, E.; Hendrikse, N.; Sleijfer, D.; Wegman, T.; Vaalburg, W.; van der Graaf, W. The distribution of drug-efflux pumps, P-gp, BCRP, MRP1 and MRP2, in the normal blood–testis barrier and in primary testicular tumours. *Eur. J. Cancer* **2004**, *40*, 2064–2070. [CrossRef] [PubMed]
144. Wakabayashi, K.; Nakagawa, H.; Tamura, A.; Koshiba, S.; Hoshijima, K.; Komada, M.; Ishikawa, T. Intramolecular disulfide bond is a critical check point determining degradative fates of ATP-binding cassette (ABC) transporter ABCG2 protein. *J. Biol. Chem.* **2007**, *282*, 27841–27846. [CrossRef] [PubMed]
145. Cooray, H.C.; Blackmore, C.G.; Maskell, L.; Barrand, M.A. Localisation of breast cancer resistance protein in microvessel endothelium of human brain. *NeuroReport* **2002**, *13*, 2059–2063. [CrossRef]
146. Basseville, A.; Hall, M.D.; Chau, C.H.; Robey, R.W.; Gottesman, M.; Figg, W.D.; Bates, S.E. The ABCG2 Multidrug Transporter. In *ABC Transporters—40 Years on*; George, A., Ed.; Springer: Cham, Switzerland, 2015; pp. 195–226. [CrossRef]
147. Stummer, W.; Koch, R.; Valle, R.D.; Roberts, D.W.; Sanai, N.; Kalkanis, S.; Hadjipanayis, C.G.; Molina, E.S. Intraoperative fluorescence diagnosis in the brain: A systematic review and suggestions for future standards on reporting diagnostic accuracy and clinical utility. *Acta Neurochir.* **2019**, *161*, 2083–2098. [CrossRef] [PubMed]
148. Diestra, J.E.; Scheffer, G.L.; Català, I.; Maliepaard, M.; Schellens, J.H.M.; Scheper, R.J.; Germà-Lluch, J.R.; Izquierdo, M.A. Frequent expression of the multi-drug resistance-associated protein BCRP/MXR/ABCP/ABCG2 in human tumours detected by the BXP-21 monoclonal antibody in paraffin-embedded material. *J. Pathol.* **2002**, *198*, 213–219. [CrossRef]
149. Barron, G.A.; Moseley, H.; Woods, J.A. Differential sensitivity in cell lines to photodynamic therapy in combination with ABCG2 inhibition. *J. Photochem. Photobiol. B: Biol.* **2013**, *126*, 87–96. [CrossRef] [PubMed]
150. Tamura, A.; Onishi, Y.; An, R.; Koshiba, S.; Wakabayashi, K.; Hoshijima, K.; Priebe, W.; Yoshida, T.; Kometani, S.; Matsubara, T.; et al. In vitro evaluation of photosensitivity risk related to genetic polymorphisms of human abc transporter abcg2 and inhibition by drugs. *Drug Metab. Pharmacokinet.* **2007**, *22*, 428–440. [CrossRef] [PubMed]
151. Kawai, N.; Hirohashi, Y.; Ebihara, Y.; Saito, T.; Murai, A.; Saito, T.; Shirosaki, T.; Kubo, T.; Nakatsugawa, M.; Kanaseki, T.; et al. ABCG2 expression is related to low 5-ALA photodynamic diagnosis (PDD) efficacy and cancer stem cell phenotype, and suppression of ABCG2 improves the efficacy of PDD. *PLoS ONE* **2019**, *14*, e0216503. [CrossRef] [PubMed]
152. Sun, W.; Kajimoto, Y.; Inoue, H.; Miyatake, S.-I.; Ishikawa, T.; Kuroiwa, T. Gefitinib enhances the efficacy of photodynamic therapy using 5-aminolevulinic acid in malignant brain tumor cells. *Photodiagn. Photodyn. Ther.* **2013**, *10*, 42–50. [CrossRef] [PubMed]
153. Liu, W.; Baer, M.R.; Bowman, M.J.; Pera, P.; Zheng, X.; Morgan, J.; Pandey, R.A.; Oseroff, A.R. The tyrosine kinase inhibitor imatinib mesylate enhances the efficacy of photodynamic therapy by inhibiting ABCG2. *Clin. Cancer Res.* **2007**, *13*, 2463–2470. [CrossRef]
154. Fujita, H.; Nagakawa, K.; Kobuchi, H.; Ogino, T.; Kondo, Y.; Inoue, K.; Shuin, T.; Utsumi, T.; Utsumi, K.; Sasaki, J.; et al. Phytoestrogen Suppresses Efflux of the Diagnostic Marker Protoporphyrin IX in Lung Carcinoma. *Cancer Res.* **2016**, *76*, 1837–1846. [CrossRef]
155. Reinert, M.; Piffaretti, D.; Wilzbach, M.; Hauger, C.; Guckler, R.; Marchi, F.; D'Angelo, M.L. Quantitative Modulation of PpIX Fluorescence and Improved Glioma Visualization. *Front. Surg.* **2019**, *6*, 41. [CrossRef] [PubMed]
156. Pick, A.; Wiese, M. Tyrosine kinase inhibitors influence ABCG2 Expression in EGFR-Positive MDCK BCRP cells via the PI3K/Akt signaling pathway. *ChemMedChem* **2012**, *7*, 650–662. [CrossRef]
157. Ahmed-Belkacem, A.; Pozza, A.; Muñoz-Martínez, F.; Bates, S.E.; Castanys, S.; Gamarro, F.; Di Pietro, A.; Pérez-Victoria, J.M. Flavonoid structure-activity studies identify 6-Prenylchrysin and tectochrysin as potent and specific inhibitors of breast cancer resistance protein ABCG2. *Cancer Res.* **2005**, *65*, 4852–4860. [CrossRef]

158. Elkind, N.K.; Szentpétery, Z.; Apáti, A.; Özvegy-Laczka, C.; Várady, G.; Ujhelly, O.; Szabó, K.; Homolya, L.; Váradi, A.; Buday, L.; et al. Multidrug Transporter ABCG2 Prevents Tumor Cell Death Induced by the Epidermal Growth Factor Receptor Inhibitor Iressa (ZD1839, Gefitinib). *Cancer Res.* **2005**, *65*, 1770–1777. [CrossRef] [PubMed]
159. Zhang, S.; Yang, X.; Coburn, R.A.; Morris, M.E. Structure activity relationships and quantitative structure activity relationships for the flavonoid-mediated inhibition of breast cancer resistance protein. *Biochem. Pharmacol.* **2005**, *70*, 627–639. [CrossRef]
160. Guo, L.; Zheng, P.; Fan, H.; Wang, H.; Xu, W.; Zhou, W. Ultrasound reverses chemoresistance in breast cancer stem cell like cells by altering ABCG2 expression. *Biosci. Rep.* **2017**, *37*, BSR20171137. [CrossRef]
161. Higuchi, T.; Yamaguchi, F.; Asakura, T.; Yoshida, D.; Oishi, Y.; Morita, A. Ultrasound Modulates Fluorescence Strength and ABCG2 mRNA Response to Aminolevulinic Acid in Glioma Cells. *J. Nippon. Med. Sch.* **2021**, *87*, 310–317. [CrossRef] [PubMed]
162. Wang, W.; Tabu, K.; Hagiya, Y.; Sugiyama, Y.; Kokubu, Y.; Murota, Y.; Ogura, S.-I.; Taga, T. Enhancement of 5-aminolevulinic acid-based fluorescence detection of side population-defined glioma stem cells by iron chelation. *Sci. Rep.* **2017**, *7*, 42070. [CrossRef] [PubMed]
163. Zutz, A.; Gompf, S.; Schägger, H.; Tampé, R. Mitochondrial ABC proteins in health and disease. *Biochim. Biophys. Acta* **2009**, *1787*, 681–690. [CrossRef]
164. Tamura, A.; An, R.; Hagiya, Y.; Hoshijima, K.; Yoshida, T.; Mikuriya, K.; Ishikawa, T. Drug-induced phototoxicity evoked by inhibition of human ABC transporter ABCG2: Development ofin vitrohigh-speed screening systems. *Expert Opin. Drug Metab. Toxicol.* **2008**, *4*, 255–272. [CrossRef]
165. Matsuo, H.; Takada, T.; Ichida, K.; Nakamura, T.; Nakayama, A.; Ikebuchi, Y.; Ito, K.; Kusanagi, Y.; Chiba, T.; Tadokoro, S.; et al. Common defects of ABCG2, a high-capacity urate exporter, cause gout: A function-based genetic analysis in a Japanese population. *Sci. Transl. Med.* **2009**, *1*, 5ra11. [CrossRef] [PubMed]
166. Krishnamurthy, P.C.; Du, G.; Fukuda, Y.; Sun, D.; Sampath, J.; Mercer, K.E.; Wang, J.; Sosa-Pineda, B.; Murti, K.G.; Schuetz, J.D. Identification of a mammalian mitochondrial porphyrin transporter. *Nature* **2006**, *443*, 586–589. [CrossRef]
167. Kitajima, Y.; Ishii, T.; Kohda, T.; Ishizuka, M.; Yamazaki, K.; Nishimura, Y.; Tanaka, T.; Dan, S.; Nakajima, M. Mechanistic study of PpIX accumulation using the JFCR39 cell panel revealed a role for dynamin 2-mediated exocytosis. *Sci. Rep.* **2019**, *9*, 8666. [CrossRef] [PubMed]
168. Zhou, S.; Zong, Y.; Ney, P.A.; Nair, G.; Stewart, C.F.; Sorrentino, B.P. Increased expression of the Abcg2 transporter during erythroid maturation plays a role in decreasing cellular protoporphyrin IX levels. *Blood* **2005**, *105*, 2571–2576. [CrossRef] [PubMed]
169. Hagiya, Y.; Fukuhara, H.; Matsumoto, K.; Endo, Y.; Nakajima, M.; Tanaka, T.; Okura, I.; Kurabayashi, A.; Furihata, M.; Inoue, K.; et al. Expression levels of PEPT1 and ABCG2 play key roles in 5-aminolevulinic acid (ALA)-induced tumor-specific protoporphyrin IX (PpIX) accumulation in bladder cancer. *Photodiagn. Photodyn. Ther.* **2013**, *10*, 288–295. [CrossRef] [PubMed]
170. Kaneko, S. Photodynamic Applications Using Aminolevulinic Acid in Neurosurgery. In *5-Aminolevulinic Acid Science, Technology and Application*; Okura, I., Tanaka, T.E., Eds.; SBI ALApromo Co., Ltd.: Tokyo, Japan; Tokyo Institute of Technology Press: Tokyo, Japan, 2012.
171. Ferreira, G.C.; Franco, R.; Lloyd, S.G.; Moura, I.; Moura, J.J.G.; Huynh, B.H. Structure and function of ferrochelatase. *J. Bioenerg. Biomembr.* **1995**, *27*, 221–229. [CrossRef]
172. Miyake, M.; Ishii, M.; Kawashima, K.; Kodama, T.; Sugano, K.; Fujimoto, K.; Hirao, Y. siRNA-mediated knockdown of the heme synthesis and degradation pathways: Modulation of treatment effect of 5-aminolevulinic acid-based photodynamic therapy in urothelial cancer cell lines. *Photochem. Photobiol.* **2009**, *85*, 1020–1027. [CrossRef] [PubMed]
173. Yang, X.; Li, W.; Palasuberniam, P.; Myers, K.A.; Wang, C.; Chen, B. Effects of Silencing Heme Biosynthesis Enzymes on 5-Aminolevulinic Acid-mediated Protoporphyrin IX Fluorescence and Photodynamic Therapy. *Photochem. Photobiol.* **2015**, *91*, 923–930. [CrossRef]
174. Poggiali, E.; Cassinerio, E.; Zanaboni, L.; Cappellini, M.D. An update on iron chelation therapy. *Blood Transfus.* **2012**, *10*, 411–422. [CrossRef]
175. Ballas, S.K.; Zeidan, A.M.; Duong, V.H.; Deveaux, M.; Heeney, M.M. The effect of iron chelation therapy on overall survival in sickle cell disease and β-thalassemia: A systematic review. *Am. J. Hematol.* **2018**, *93*, 943–952. [CrossRef]
176. Iinuma, S.; Farshi, S.S.; Ortel, B.; Hasan, T.N. A mechanistic study of cellular photodestruction with 5-aminolaevulinic acid-induced porphyrin. *Br. J. Cancer* **1994**, *70*, 21–28. [CrossRef]
177. Juzenas, P.; Juzeniene, A.; Moan, J. Deferoxamine photosensitizes cancer cells in vitro. *Biochem. Biophys. Res. Commun.* **2005**, *332*, 388–391. [CrossRef] [PubMed]
178. Lin, F.; Geiger, P.G.; Korytowski, W.; Girotti, A.W. Protoporphyrin IX-sensitized photoinactivation of 5-aminolevulinate-treated leukemia cells: Effects of exogenous iron. *Photochem. Photobiol.* **1999**, *69*, 375–381. [CrossRef]
179. Uekusa, M.; Omura, K.; Nakajima, Y.; Hasegawa, S.; Harada, H.; Morita, K.-I.; Tsuda, H. Uptake and kinetics of 5-aminolevulinic acid in oral squamous cell carcinoma. *Int. J. Oral Maxillofac. Surg.* **2010**, *39*, 802–805. [CrossRef] [PubMed]
180. Tan, W.C.; Krasner, N.; O'Toole, P.; Lombard, M. Enhancement of photodynamic therapy in gastric cancer cells by removal of iron. *Gut* **1997**, *41*, 14–18. [CrossRef]
181. Berg, K.; Anholt, H.; Bech, O.; Moan, J. The influence of iron chelators on the accumulation of protoporphyrin IX in 5-aminolaevulinic acid-treated cells. *Br. J. Cancer* **1996**, *74*, 688–697. [CrossRef]
182. Yang, J.; Xia, Y.; Liu, X.; Jiang, S.; Xiong, L. Desferrioxamine shows different potentials for enhancing 5-aminolaevulinic acid-based photodynamic therapy in several cutaneous cell lines. *Lasers Med. Sci.* **2010**, *25*, 251–257. [CrossRef]

183. Inoue, K.; Fukuhara, H.; Kurabayashi, A.; Furihata, M.; Tsuda, M.; Nagakawa, K.; Fujita, H.; Utsumi, K.; Shuin, T. Photodynamic therapy involves an antiangiogenic mechanism and is enhanced by ferrochelatase inhibitor in urothelial carcinoma. *Cancer Sci.* **2013**, *104*, 765–772. [CrossRef] [PubMed]
184. Valdés, P.A.; Samkoe, K.; O'Hara, J.A.; Roberts, D.W.; Paulsen, K.D.; Pogue, B.W. Deferoxamine iron chelation increases δ-aminolevulinic acid induced protoporphyrin IX in xenograft glioma model. *Photochem. Photobiol.* **2010**, *86*, 471–475. [CrossRef]
185. Choudry, K.; Brooke, R.; Farrar, W.; Rhodes, L. The effect of an iron chelating agent on protoporphyrin IX levels and phototoxicity in topical 5-aminolaevulinic acid photodynamic therapy. *Br. J. Dermatol.* **2003**, *149*, 124–130. [CrossRef]
186. De Matteis, F.; Dawson, S.J.; Pons, N.; Pipino, S. Bilirubin and uroporphyrinogen oxidation by induced cytochrome P4501A and cytochrome P4502B: Role of polyhalogenated biphenyls of different configuration. *Biochem. Pharmacol.* **2002**, *63*, 615–624. [CrossRef]
187. Hou, J.; Cai, S.; Kitajima, Y.; Fujino, M.; Ito, H.; Takahashi, K.; Abe, F.; Tanaka, T.; Ding, Q.; Li, X.-K. 5-Aminolevulinic acid combined with ferrous iron induces carbon monoxide generation in mouse kidneys and protects from renal ischemia-reperfusion injury. *Am. J. Physiol. Renal Physiol.* **2013**, *305*, F1149–F1157. [CrossRef] [PubMed]
188. Jozkowicz, A.; Was, H.; Dulak, J. Heme Oxygenase-1 in Tumors: Is It a False Friend? *Antioxid. Redox Signal.* **2007**, *9*, 2099–2117. [CrossRef]
189. Tenhunen, R.; Marver, H.S.; Schmid, R. The enzymatic conversion of heme to bilirubin by microsomal heme oxygenase. *Proc. Natl. Acad. Sci. USA* **1968**, *61*, 748–755. [CrossRef] [PubMed]
190. Ajioka, R.S.; Phillips, J.D.; Kushner, J.P. Biosynthesis of heme in mammals. *Biochim. Biophys. Acta* **2006**, *1763*, 723–736. [CrossRef] [PubMed]
191. Wilks, A.; Heinzl, G. Heme oxygenation and the widening paradigm of heme degradation. *Arch. Biochem. Biophys.* **2014**, *544*, 87–95. [CrossRef]
192. Nimura, T.; Weinstein, P.R.; Massa, S.M.; Panter, S.; Sharp, F.R. Heme oxygenase-1 (HO-1) protein induction in rat brain following focal ischemia. *Mol. Brain Res.* **1996**, *37*, 201–208. [CrossRef]
193. Fukuda, K.; Panter, S.S.; Sharp, F.R.; Noble, L. Induction of heme oxygenase-1 (HO-1) after traumatic brain injury in the rat. *Neurosci. Lett.* **1995**, *199*, 127–130. [CrossRef]
194. Schipper, H.M.; Cissé, S.; Stopa, E.G. Expression of heme oxygenase-1 in the senescent and alzheimer-diseased brain. *Ann. Neurol.* **1995**, *37*, 758–768. [CrossRef] [PubMed]
195. Sacca, P.A.; Meiss, R.; Casas, G.; Mazza, O.; Calvo, J.C.; Navone, N.M.; Vazquez, E. Nuclear translocation of haeme oxygenase-1 is associated to prostate cancer. *Br. J. Cancer* **2007**, *97*, 1683–1689. [CrossRef]
196. Maines, M.D.; Abrahamsson, P.-A. Expression of heme oxygenase-1 (HSP32) in human prostate: Normal, hyperplastic, and tumor tissue distribution. *Urology* **1996**, *47*, 727–733. [CrossRef]
197. Berberat, P.O.; Dambrauskas, Z.; Gulbinas, A.; Giese, T.; Giese, N.; Künzli, B.; Autschbach, F.; Meuer, S.; Büchler, M.W.; Friess, H. Inhibition of heme oxygenase-1 increases responsiveness of pancreatic cancer cells to anticancer treatment. *Clin. Cancer Res.* **2005**, *11*, 3790–3798. [CrossRef]
198. Torisu-Itakura, H.; Furue, M.; Kuwano, M.; Ono, M. Co-expression of thymidine phosphorylase and heme oxygenase-1 in macrophages in human malignant vertical growth melanomas. *Jpn. J. Cancer Res.* **2000**, *91*, 906–910. [CrossRef]
199. Mayerhofer, M.; Florian, S.; Krauth, M.-T.; Aichberger, K.J.; Bilban, M.; Marculescu, R.; Printz, D.; Fritsch, G.; Wagner, O.; Selzer, E.; et al. Identification of heme oxygenase-1 as a novel BCR/ABL-dependent survival factor in chronic myeloid leukemia. *Cancer Res.* **2004**, *64*, 3148–3154. [CrossRef]
200. Doi, K.; Akaike, T.; Fujii, S.; Tanaka, S.; Ikebe, N.; Beppu, T.; Shibahara, S.; Ogawa, M.; Maeda, H. Induction of haem oxygenase-1 by nitric oxide and ischaemia in experimental solid tumours and implications for tumour growth. *Br. J. Cancer* **1999**, *80*, 1945–1954. [CrossRef]
201. Schacter, B.A.; Kurz, P. Alterations in hepatic and splenic microsomal electron transport system components, drug metabolism, heme oxygenase activity, and cytochrome P-450 turnover in Murphy-Sturm lymphosarcoma-bearing rats. *Cancer Res.* **1982**, *42*, 3557–3564. [PubMed]
202. Degese, M.S.; Mendizabal, J.E.; Gandini, N.A.; Gutkind, J.S.; Molinolo, A.; Hewitt, S.; Curino, A.C.; Coso, O.A.; Facchinetti, M.M. Expression of heme oxygenase-1 in non-small cell lung cancer (NSCLC) and its correlation with clinical data. *Lung Cancer* **2012**, *77*, 168–175. [CrossRef] [PubMed]
203. Goodman, A.I.; Choudhury, M.; Da Silva, J.-L.; Schwartzman, M.L.; Abraham, N.G. Overexpression of the heme oxygenase gene in renal cell carcinoma. *Proc. Soc. Exp. Biol. Med.* **1997**, *214*, 54–75. [CrossRef]
204. Deininger, M.H.; Meyermann, R.; Trautmann, K.; Duffner, F.; Grote, E.H.; Wickboldt, J.; Schluesener, H.J. Heme oxygenase (HO)-1 expressing macrophages/microglial cells accumulate during oligodendroglioma progression. *Brain Res.* **2000**, *882*, 1–8. [CrossRef]
205. Hara, E.; Takahashi, K.; Tominaga, T.; Kumabe, T.; Kayama, T.; Suzuki, H.; Fujita, H.; Yoshimoto, T.; Shirato, K.; Shibahara, S. Expression of heme oxygenase and inducible nitric oxide synthase mRNA in human brain tumors. *Biochem. Biophys. Res. Commun.* **1996**, *224*, 153–158. [CrossRef] [PubMed]
206. El Andaloussi, A.; Lesniak, M.S. CD4+CD25+FoxP3+ T-cell infiltration and heme oxygenase-1 expression correlate with tumor grade in human gliomas. *J. Neuro-Oncol.* **2007**, *83*, 145–152. [CrossRef] [PubMed]
207. Gandini, N.A.; Fermento, M.E.; Salomón, D.G.; Obiol, D.J.; Andrés, N.C.; Zenklusen, J.C.; Arévalo, J.; Blasco, J.; Romero, A.L.; Facchinetti, M.M.; et al. Heme oxygenase-1 expression in human gliomas and its correlation with poor prognosis in patients with astrocytoma. *Tumor Biol.* **2014**, *35*, 2803–2815. [CrossRef] [PubMed]

208. Abdullah, L.N.; Chow, E.K.-H. Mechanisms of chemoresistance in cancer stem cells. *Clin. Transl. Med.* **2013**, *2*, 3. [CrossRef] [PubMed]
209. Baumann, M.; Krause, M.; Hill, R. Exploring the role of cancer stem cells in radioresistance. *Nat. Rev. Cancer* **2008**, *8*, 545–554. [CrossRef] [PubMed]
210. Frank, J.; Lornejad-Schäfer, M.R.; Schöffl, H.; Flaccus, A.; Lambert, C.; Biesalski, H.K. Inhibition of heme oxygenase-1 increases responsiveness of melanoma cells to ALA-based photodynamic therapy. *Int. J. Oncol.* **2007**, *31*, 1539–1545. [CrossRef] [PubMed]
211. Stevenson, D.K.; Wong, R.J. Metalloporphyrins in the management of neonatal hyperbilirubinemia. *Semin. Fetal Neonatal Med.* **2010**, *15*, 164–168. [CrossRef]
212. Zhang, H.; Berezov, A.; Wang, Q.; Zhang, G.; Drebin, J.; Murali, R.; Greene, M.I. ErbB receptors: From oncogenes to targeted cancer therapies. *J. Clin. Investig.* **2007**, *117*, 2051–2058. [CrossRef]
213. Arteaga, C.L. Epidermal growth factor receptordependence in human tumors: More than justexpression? *Oncologist* **2002**, *7* (Suppl. 4), 31–39. [CrossRef] [PubMed]
214. Burtness, B. The role of cetuximab in the treatment of squamous cell cancer of the head and neck. *Expert Opin. Biol. Ther.* **2005**, *5*, 1085–1093. [CrossRef]
215. Hatanpaa, K.J.; Burma, S.; Zhao, D.; Habib, A.A. Epidermal growth factor receptor in glioma: Signal transduction, neuropathology, imaging, and radioresistance. *Neoplasia* **2010**, *12*, 675–684. [CrossRef] [PubMed]
216. Frederick, L.; Wang, X.Y.; Eley, G.; James, C.D. Diversity and frequency of epidermal growth factor receptor mutations in human glioblastomas. *Cancer Res.* **2000**, *60*, 1383–1387. [PubMed]
217. Motekallemi, A.; Jeltema, H.-R.; Metzemaekers, J.D.M.; Van Dam, G.M.; Crane, L.M.A.; Groen, R.J.M. The current status of 5-ALA fluorescence-guided resection of intracranial meningiomas—A critical review. *Neurosurg. Rev.* **2015**, *38*, 619–628. [CrossRef] [PubMed]
218. Kim, J.E.; Cho, H.R.; Xu, W.J.; Kim, J.Y.; Kim, S.K.; Kim, S.-K.; Park, S.-H.; Kim, H.; Lee, S.-H.; Choi, S.H.; et al. Mechanism for enhanced 5-aminolevulinic acid fluorescence in isocitrate dehydrogenase 1 mutant malignant gliomas. *Oncotarget* **2015**, *6*, 20266–20277. [CrossRef]
219. Voldborg, B.R.; Damstrup, L.; Spang-Thomsen, M.; Poulsen, H.S. Pidermal growth factor receptor(EGFR) and EGFR mutations, function and possiblerole in clinical trials. *Ann. Oncol.* **1997**, *8*, 1197–1206. [CrossRef]
220. Jungbluth, A.A.; Stockert, E.; Huang, H.J.; Collins, V.P.; Coplan, K.; Iversen, K.; Kolb, D.; Johns, T.J.; Scott, A.M.; Gullick, W.J.; et al. A monoclonal antibodyrecognizing human cancers with amplification/overexpression of the human epidermal growth factorreceptor. *Proc. Natl. Acad. Sci. USA* **2003**, *100*, 639–644. [CrossRef] [PubMed]
221. Kuroda, H.; Takeno, M.; Murakami, S.; Miyazawa, N.; Kaneko, T.; Ishigatsubo, Y. Inhibition of heme oxygenase-1 with an epidermal growth factor receptor inhibitor and cisplatin decreases proliferation of lung cancer A549 cells. *Lung Cancer* **2010**, *67*, 31–36. [CrossRef] [PubMed]
222. Lien, G.-S.; Wu, M.-S.; Bien, M.-Y.; Chen, C.-H.; Lin, C.-H.; Chen, B.-C. Epidermal growth factor stimulates nuclear factor-κB activation and heme oxygenase-1 expression via c-Src, NADPH oxidase, PI3K, and Akt in human colon cancer cells. *PLoS ONE* **2014**, *9*, e104891. [CrossRef]
223. Biswas, D.K.; Cruz, A.P.; Gansberger, E.; Pardee, A.B. Epidermal growth factor-induced nuclear factor kappa B activation: A major pathway of cell-cycle progression in estrogen-receptor negative breast cancer cells. *Proc. Natl. Acad. Sci. USA* **2000**, *97*, 8542–8547. [CrossRef]
224. Padfield, E.; Ellis, H.P.; Kurian, K.M. Current Therapeutic Advances Targeting EGFR and EGFRvIII in Glioblastoma. *Front. Oncol.* **2015**, *5*, 5. [CrossRef]
225. Louis, D.N.; Perry, A.; Wesseling, P.; Brat, D.J.; Cree, I.A.; Figarella-Branger, D.; Hawkins, C.; Ng, H.K.; Pfister, S.M.; Reifenberger, G.; et al. The 2021 WHO Classification of Tumors of the Central Nervous System: A summary. *Neuro-Oncology* **2021**, *23*, 1231–1251. [CrossRef] [PubMed]
226. Ohba, S.; Hirose, Y. Biological Significance of Mutant Isocitrate Dehydrogenase 1 and 2 in Gliomagenesis. *Neurol. Med. Chir.* **2016**, *56*, 170–179. [CrossRef] [PubMed]
227. Xu, X.; Zhao, J.; Xu, Z.; Peng, B.; Huang, Q.; Arnold, E.; Ding, J. Structures of human cytosolic NADP-dependent isocitrate dehydrogenase reveal a novel self-regulatory mechanism of activity. *J. Biol. Chem.* **2004**, *279*, 33946–33957. [CrossRef]
228. Leonardi, R.; Subramanian, C.; Jackowski, S.; Rock, C.O. Cancer-associated isocitrate dehydrogenase mutations inactivate nadph-dependent reductive carboxylation. *J. Biol. Chem.* **2012**, *287*, 14615–14620. [CrossRef]
229. Collaud, S.; Juzeniene, A.; Moan, J.; Lange, N. On the Selectivity of 5-Aminolevulinic Acid-Induced Protoporphyrin IX Formation. *Curr. Med. Chem. Agents* **2004**, *4*, 301–316. [CrossRef] [PubMed]
230. Abraham, N.G.; Kappas, A. Pharmacological and clinical aspects of heme oxygenase. *Pharmacol. Rev.* **2008**, *60*, 79–127. [CrossRef]
231. Sanson, M.; Marie, Y.; Paris, S.; Idbaih, A.; Laffaire, J.; Ducray, F.; El Hallani, S.; Boisselier, B.; Mokhtari, K.; Hoang-Xuan, K.; et al. Isocitrate dehydrogenase 1 codon 132 mutation is an important prognostic biomarker in gliomas. *J. Clin. Oncol.* **2009**, *27*, 4150–4154. [CrossRef] [PubMed]
232. Ward, P.; Cross, J.; Lu, C.; Weigert, O.; Abel-Wahab, O.; Levine, R.L.; Weinstock, D.M.; Sharp, K.A.; Thompson, C.B. Identification of additional IDH mutations associated with oncometabolite R(−)-2-hydroxyglutarate production. *Oncogene* **2011**, *31*, 2491–2498. [CrossRef] [PubMed]
233. Dang, L.; White, D.W.; Gross, S.; Bennett, B.D.; Bittinger, M.A.; Driggers, E.M.; Fantin, V.R.; Jang, H.G.; Jin, S.; Keenan, M.C.; et al. Cancer-associated IDH1 mutations produce 2-hydroxyglutarate. *Nature* **2009**, *462*, 739–744. [CrossRef] [PubMed]

234. Yano, H.; Nakayama, N.; Hirose, Y.; Ohe, N.; Shinoda, J.; Yoshimura, S.-I.; Iwama, T. Intraventricular glioneuronal tumor with disseminated lesions at diagnosis—A case report. *Diagn. Pathol.* **2011**, *6*, 119. [CrossRef] [PubMed]
235. Bleeker, F.E.; Atai, N.A.; Lamba, S.; Jonker, A.; Rijkeboer, D.; Bosch, K.S.; Tigchelaar, W.; Troost, D.; Vandertop, W.P.; Bardelli, A.; et al. The prognostic IDH1 R132 mutation is associated with reduced NADP+-dependent IDH activity in glioblastoma. *Acta Neuropathol.* **2010**, *119*, 487–494. [CrossRef] [PubMed]
236. Hickmann, A.-K.; Nadji-Ohl, M.; Hopf, N.J. Feasibility of fluorescence-guided resection of recurrent gliomas using five-aminolevulinic acid: Retrospective analysis of surgical and neurological outcome in 58 patients. *J. Neuro-Oncol.* **2015**, *122*, 151–160. [CrossRef] [PubMed]
237. Boroughs, L.K.; DeBerardinis, R.J. Metabolic pathways promoting cancer cell survival and growth. *Nat. Cell Biol.* **2015**, *17*, 351–359. [CrossRef] [PubMed]
238. Fan, J.; Ye, J.; Kamphorst, J.; Shlomi, T.; Thompson, C.B.; Rabinowitz, J.D. Quantitative flux analysis reveals folate-dependent NADPH production. *Nature* **2014**, *510*, 298–302. [CrossRef] [PubMed]
239. Abraham, N.G.; Lin, J.H.; Dunn, M.W.; Schwartzman, M.L. Presence of heme oxygenase and NADPH cytochrome P-450 (c) reductase in human corneal epithelium. *Investig. Ophthalmol. Vis. Sci.* **1987**, *28*, 1464–1472.
240. Atai, N.A.; Renkema-Mills, N.A.; Bosman, J.; Schmidt, N.; Rijkeboer, D.; Tigchelaar, W.; Bosch, K.S.; Troost, D.; Jonker, A.; Bleeker, F.E.; et al. Differential activity of nadph-producing dehydrogenases renders rodents unsuitable models to study idh1r132 mutation effects in human glioblastoma. *J. Histochem. Cytochem.* **2011**, *59*, 489–503. [CrossRef] [PubMed]
241. Wahl, D.R.; Dresser, J.; Wilder-Romans, K.; Parsels, J.D.; Zhao, S.G.; Davis, M.; Zhao, L.; Kachman, M.; Wernisch, S.; Burant, C.F.; et al. Glioblastoma Therapy Can Be Augmented by Targeting IDH1-Mediated NADPH Biosynthesis. *Cancer Res.* **2017**, *77*, 960–970. [CrossRef]
242. Hu, W.; Zhang, C.; Wu, R.; Sun, Y.; Levine, A.; Feng, Z. Glutaminase 2, a novel p53 target gene regulating energy metabolism and antioxidant function. *Proc. Natl. Acad. Sci. USA* **2010**, *107*, 7455–7460. [CrossRef]
243. Suzuki, S.; Tanaka, T.; Poyurovsky, M.V.; Nagano, H.; Mayama, T.; Ohkubo, S.; Lokshin, M.; Hosokawa, H.; Nakayama, T.; Suzuki, Y.; et al. Phosphate-activated glutaminase (GLS2), a p53-inducible regulator of glutamine metabolism and reactive oxygen species. *Proc. Natl. Acad. Sci. USA* **2010**, *107*, 7461–7466. [CrossRef]
244. Szeliga, M.; Albrecht, J. Opposing roles of glutaminase isoforms in determining glioblastoma cell phenotype. *Neurochem. Int.* **2015**, *88*, 6–9. [CrossRef] [PubMed]
245. Marcus, H.J.; Carpenter, K.L.H.; Price, S.J.; Hutchinson, P.J. In vivo assessment of high-grade glioma biochemistry using microdialysis: A study of energy-related molecules, growth factors and cytokines. *J. Neuro-Oncol.* **2010**, *97*, 11–23. [CrossRef]
246. Xiang, L.; Xie, G.; Liu, C.; Zhou, J.; Chen, J.; Yu, S.; Li, J.; Pang, X.; Shi, H.; Liang, H. Knock-down of glutaminase 2 expression decreases glutathione, NADH, and sensitizes cervical cancer to ionizing radiation. *Biochim. Biophys. Acta* **2013**, *1833*, 2996–3005. [CrossRef] [PubMed]
247. DeBerardinis, R.J.; Cheng, T. Q's next: The diverse functions of glutamine in metabolism, cell biology and cancer. *Oncogene* **2010**, *29*, 313–324. [CrossRef]
248. Szeliga, M.; Sidoryk, M.; Matyja, E.; Kowalczyk, P.; Albrecht, J. Lack of expression of the liver-type glutaminase (LGA) mRNA in human malignant gliomas. *Neurosci. Lett.* **2005**, *374*, 171–173. [CrossRef] [PubMed]
249. Szeliga, M.; Bogacińska-Karaś, M.; Kuzmicz-Kowalska, K.; Rola, R.; Albrecht, J. Downregulation of GLS2 in glioblastoma cells is related to DNA hypermethylation but not to the p53 status. *Mol. Carcinog.* **2016**, *55*, 1309–1316. [CrossRef] [PubMed]
250. Szeliga, M.; Obara-Michlewska, M.; Matyja, E.; Łazarczyk, M.; Lobo, C.; Hilgier, W.; Alonso, F.J.; Márquez, J.; Albrecht, J. Transfection with liver-type glutaminase cDNA alters gene expression and reduces survival, migration and proliferation of T98G glioma cells. *Glia* **2009**, *57*, 1014–1023. [CrossRef] [PubMed]
251. Moots, P.L.; Maciunas, R.J.; Eisert, D.R.; Parker, R.A.; Laporte, K.; Abou-Khalil, B. The course of seizure disorders in patients with malignant gliomas. *Arch. Neurol.* **1995**, *52*, 717–724. [CrossRef] [PubMed]
252. Nabavi, A.; Thurm, H.; Zountsas, B.; Pietsch, T.; Lanfermann, H.; Pichlmeier, U.; Mehdorn, M. Five-aminolevulinic acid for fluorescence-guided resection of recurrent malignant gliomas. *Neurosurgery* **2009**, *65*, 1070–1077. [CrossRef]
253. Kurzwelly, D.; Herrlinger, U.; Simon, M. Seizures in patients with low-grade gliomas—Incidence, pathogenesis, surgical management, and pharmacotherapy. *Adv. Tech. Stand. Neurosurg.* **2010**, *35*, 81–111. [CrossRef] [PubMed]
254. Hirsch, L. Seizures in patients undergoing resection of low-grade gliomas. *Epilepsy Curr.* **2009**, *9*, 98–100. [CrossRef]
255. Rudà, R.; Bello, L.; Duffau, H.; Soffietti, R. Seizures in low-grade gliomas: Natural history, pathogenesis, and outcome after treatments. *Neuro-Oncology* **2012**, *14* (Suppl. 4), iv55–iv64. [CrossRef] [PubMed]
256. Rosati, A.; Buttolo, L.; Stefini, R.; Todeschini, A.; Cenzato, M.; Padovani, A. Efficacy and safety of levetiracetam in patients with glioma. *Arch. Neurol.* **2010**, *67*, 343–346. [CrossRef] [PubMed]
257. Ständer, M.; Dichgans, J.; Weller, M. Anticonvulsant drugs fail to modulate chemotherapy-induced cytotoxicity and growth inhibition of human malignant glioma cells. *J. Neuro-Oncol.* **1998**, *37*, 191–198. [CrossRef]
258. Usery, J.B.; Michael, L.M.; Sills, A.K.; Finch, C. A prospective evaluation and literature review of levetiracetam use in patients with brain tumors and seizures. *J. Neuro-Oncol.* **2010**, *99*, 251–260. [CrossRef]
259. Lawrence, J.E.; Steele, C.J.; Rovin, R.A.; Belton, R.J.; Winn, R.J. Dexamethasone alone and in combination with desipramine, phenytoin, valproic acid or levetiracetam interferes with 5-ALA-mediated PpIX production and cellular retention in glioblastoma cells. *J. Neuro-Oncol.* **2016**, *127*, 15–21. [CrossRef] [PubMed]

260. Underwood, J.L.; Murphy, C.G.; Chen, J.; Franse-Carman, L.; Wood, I.; Epstein, D.L.; Alvarado, J.A. Glucocorticoids regulate transendothelial fluid flow resistance and formation of intercellular junctions. *Am. J. Physiol.* **1999**, *277*, C330–C342. [CrossRef]
261. Tonn, J.-C.; Stummer, W. Fluorescence-guided resection of malignant gliomas using 5-aminolevulinic acid: Practical use, risks, and pitfalls. *Clin. Neurosurg.* **2008**, *55*, 20–26.
262. Hefti, M.; Albert, I.; Luginbuehl, V. Phenytoin reduces 5-aminolevulinic acid-induced protoporphyrin IX accumulation in malignant glioma cells. *J. Neuro-Oncol.* **2012**, *108*, 443–450. [CrossRef]
263. Santos, N.; Medina, W.; Martins, N.; Mingatto, F.; Curti, C.; Santos, A. Aromatic antiepileptic drugs and mitochondrial toxicity: Effects on mitochondria isolated from rat liver. *Toxicol. In Vitro* **2008**, *22*, 1143–1152. [CrossRef] [PubMed]
264. Meyer, R.P.; Knoth, R.; Schiltz, E.; Volk, B. Possible function of astrocyte cytochrome p450 in control of xenobiotic phenytoin in the brain: In vitro studies on murine astrocyte primary cultures. *Exp. Neurol.* **2001**, *167*, 376–384. [CrossRef]
265. Haust, H.L.; Poon, H.C.; Carson, R.; Vandewetering, C.; Peter, F. Protoporphyrinaemia and decreased activities of 5-aminolevulinic acid dehydrase and uroporphyrinogen I synthetase in erythrocytes of a vitamin B6-deficient epileptic boy given valproic acid and carbamazepine. *Clin. Biochem.* **1989**, *22*, 201–211. [CrossRef]
266. Kamp, M.A.; Knipps, J.; Neumann, L.M.; Mijderwijk, H.-J.; Dibué-Adjei, M.; Steiger, H.-J.; Slotty, P.J.; Rapp, M.; Cornelius, J.-F.; Sabel, M. Is the Intensity of 5-Aminolevulinic Acid–Derived Fluorescence Related to the Light Source? *World Neurosurg.* **2019**, *131*, e271–e276. [CrossRef] [PubMed]
267. Belykh, E.; Nelson, L.Y.; Seibel, E.J.; Preul, M.C. Letter to the Editor: Factors that Influence Quantification of Fluorescent Signal during the 5-ALA-Guided Surgery. *World Neurosurg.* **2020**, *139*, 700–702. [CrossRef] [PubMed]
268. Belykh, E.; Miller, E.J.; Patel, A.A.; Bozkurt, B.; Yağmurlu, K.; Robinson, T.R.; Nakaji, P.; Spetzler, R.F.; Lawton, M.T.; Nelson, L.Y.; et al. Optical Characterization of Neurosurgical Operating Microscopes: Quantitative Fluorescence and Assessment of PpIX Photobleaching. *Sci. Rep.* **2018**, *8*, 12543. [CrossRef] [PubMed]